Numerical Investigation of Spin-Up of a Fluid-Filled Cylindrical Tank

Validation of FINE/Open with OpenLabs and DrNUM

Dennis Kröger

A thesis presented for the degree of
Engineering physics

LUND UNIVERSITY

Energy Science
Lunds University
Sweden

2018-05-31

This degree project for the degree Master of Science in Engineering has been conducted at the Division of Fluid Mechanics, Department of Energy Science, Faculty of Engineering, Lunds University, and at the European Space Research and Technology Centre (ESTEC), The Netherlands.

Supervisor at the Division of Fluid Mechanics was Professor Johan Revstedt.
Supervisor at ESTEC was Richard Schwane.
Examiner at Lunds University was Professor Xuo-Song Bai.
The project was carried out in cooperation with Master's Student in Mechanical Engineering, Jakob Svensson.

Thesis for the Degree of Master of Science in Engineering
ISRN LUTMDN/TMHP-18/5404-SE
ISSN 0282-1990

Fluid Mechanics
Department of Energy Science
Faculty of Engineering, Lund University
Sweden
www.energy.lth.se

Abstract

This report is an investigation on how well fuel sloshing in a rotating cylindrical tank can be modeled numerically. The investigation is motivated by the need to understand the fuel sloshing in the new Ariane 6 rocket developed by the European Space Agency. Two cases are studied, the filled tank and the half filled tank at Reynolds numbers of 71000-212000. The softwares studied are FINE/Open with OpenLabs from Numeca and DrNUM from enGits. For the filled tank, the softwares are able to capture the main characteristics of the flow development such as the rotational velocities and a secondary flow developed during spin-up which is known as the Ekman pumping. The time to reach a solid body rotating is investigated and compared with experimental and theoretical data. The comparison showed that the spin-up time is not predicted correctly.
The free surface of a half filled tank introduces a lot of instabilities and numerically difficulties. Stable simulations are achieved but no solid body rotation is reached.

Acknowledgement

This project was carried out at the European Space Research and Technology Centre in The Netherlands, Noordwijk. I want to thank Master student Jakob Svensson whom I have been sharing an office with during my time at ESTEC. We constantly came up with new ideas during discussions on how to develop and improve the project. I want to thank Henrike Jakob who started working on this project.

A thanks goes to Diebert Van Rhijn for his IT support, without it most of the results in this project would not be possible. I also want to thank Ronan Flanagan for his numerical support and simulations.

A special thanks to my supervisor Richard Schwane who gave me the opportunity to work on this project. We had a lot of great discussions that helped to shape the project. And a big thanks to all the interns that made my time at ESTEC truly memorable.

Contents

List of Figures

List of Tables

Abbreviations

CFD, Computational Fluid Dynamics
SBR, Solid Body Rotation
PIV, Particle Image Velocimetry
LH2, Liquid hydrogen
CPU, Central Processing Unit
GPU, Graphics Processing Unit

List of Symbols

ρ, Density
p, Pressure
μ, Kinematic viscosity, [m^2/s]
Ω, Radial velocity, [rad/s]
c, Half height of the tank, [m]
E, Ekman number
v, velocity [m/s]
r, radial component, [m]
$\vec{V}$, Velocity vector
$\frac{D}{DT}$, Substantial derivative
τ, Tangential stresses [N/m^2]
f, Force [N]
q, Heat flux [W/m^2]
Δt, Time step [s]
Δx, Cell size [m]
R, Cylinder radius [m]
A_{sim}, Area under simulated velocity profile [m^2]
A_{sbr}, Area under linear velocity profile [m^2]
λ, Evolution criteria
U^n, U at time t
U^{n+1}, U at time t+$\triangle$ t
α, Runge-Kutta coefficients

1 Introduction

This research is motivated by the need to numerically model the fuel sloshing in the upper stage tank of the new Ariane 6 rocket.

The new Ariane 6 rocket will have multiple satellites as its payload which are deployed at different orbital stages. This requires that the engine can be stopped and started again in micro-gravity conditions. The new Vinci engine of Ariane 6 is already capable of doing that [1] but in order for the engine to function it needs to have fuel accessible at all time. To ensure fuel accessibility at all time the fuels behavior during the upper stage needs to be understood. An additional criteria is that the fuel entering the engine can't contain any bubbles. An air bubble of only 1 cm^3 entering the engine would cause a complete break down. [2]
After the acceleration phase of the flight the coasting phase is begun where the partially filled tank will be exposed to micro-gravity conditions. This coasting phase will last for more than a month. In order to stabilize the coasting the rocket will begin to rotate around its own center axis. This rotation causes the fuel to reach Reynolds numbers up to 1250000. The rotation will cause multiple tons of fuel to slosh around in the tank. The force of this sloshing will cause the rocket to destabilize. In order to counter steer the forces caused by the sloshing it would need to burn all of it's fuel in a matter of weeks. [2] Clearly this is not a sustainable solution and therefore a lot of research has started to address this problem.

1.1 Problem description

It is extremely expensive to conduct research and set up experiments in space. For this reason the upper stage condition have been simplified down to a level which makes it possible to study it on earth. The goal is to recreate at least some of the effects and issues that can appear in the upper stage tank under real conditions.

Two CFD softwares are used and validated. The main CFD software is FINE/Open with OpenLabs from Numeca. This is a more advanced code that is supposed to be able to deal with a lot of upper stage conditions such as cryogenic fluids and free surface reorientation. [3]

The second software used is DrNUM. DrNUM is a new CFD software being developed by enGits GmbH and numrax GmbH. It was released to the public in 2013. [4] The software is compiled to run on a GPU. This gives a great advantage in terms of computational power and is the reason why this software is tested in addition to FINE/Open with OpenLabs.

Several commercial CFD solvers have been tested before this research for similar problems but found to lack some of the needed physical models to correctly describe the fuel sloshing in micro-gravity at high rotational speed. [5][6]

Modeling the fuel sloshing under real conditions as in the coasting phase of the Ariane 6 rocket is a hugely complex problem and out of scope for a master thesis. This research will serve as a first step to assess the CFD solvers and their capability to model fuel sloshing under simplified condition.

Before modeling the cylindrical tank a short study on the driven cavity problem is performed and can be found in appendix A. The driven cavity problem is a highly validated case and is a good way to determine a solvers capability to model fluids at higher Reynolds numbers. The results from the study are found satisfying and with good agreement with existing literature.

The second step of validation is to determine the capability of the mentioned CFD solvers to model the spin-up of a cylindrical tank under greatly simplified conditions.

The problem is simplified down to an isothermal case with a low rotational speed, water as the fluid and ground conditions. The geometry of the tank is also simplified down to the geometry seen in figure 1.

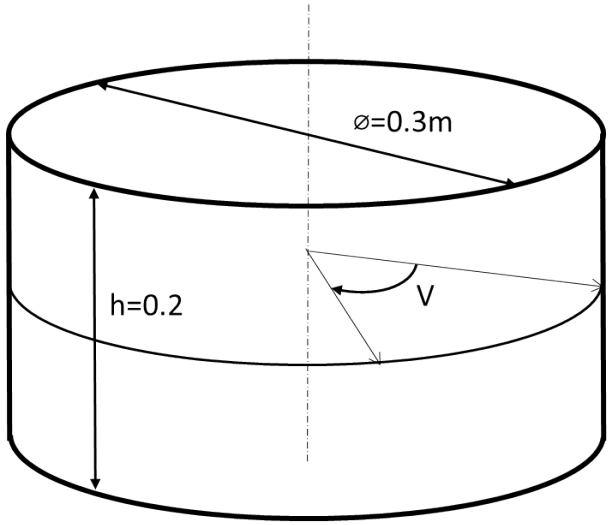

Figure 1: The tank geometry studied in this project.

The tank has a diameter of 0.3m and a height of 0.2m. The numerical results from FINE/Open with OpenLabs are compared with experimental results based on the same geometry.
The experimental work is run in parallel to this work and is performed by master student in Mechanical Engineering Jakob Svensson [7].

2 Theory

Before going into the numerical part of the study it is important to have a good understanding of the basic physics behind such a case. This will help to understand, and determine the validity of the computed results. In this section the main physical phenomena involved in a spin-up of a cylindrical tank are formulated.

Furthermore a brief discussion of the theory behind computing fluid dynamics is given.

2.1 Physics

Even though the geometry of the studied case is simplified, the flow developing as the cylinder is spinning up can become quite complex. It is shown that secondary flows are building up as the tank is accelerated. These secondary flows are shown to be a dominating factor to reach a solid body rotation, SBR. [8]
The fluid studied for all cases is water. In a real life application the water is replaced with liquid hydrogen but for experimental purposes water is much more convenient. All the simplifications made to the case are summarized in table 3 in the setup section.
Two cases are studied in this research, the full tank and half filled tank. The full tank case is filled with water with no second fluid in the tank. For the half filled tank case, half of the tank is filled with water and the rest is air. These two cases have a lot of similarities in the build up of the flow regime. But there are some additional physical phenomena that need to be taken into account as soon as a free surface is studied.
The spin-up for a full tank is discussed in the following section and later on expanded to a half filled tank.

2.1.1 Full tank

The initial state is always considered from rest i.e. the tank has no rotational speed and there are no velocity components in the fluid. This is a simplification made in order to better compare the results to the experiments.

As the walls are set to a rotational speed the fluid close to the walls gets accelerated due to viscous forces. This flow can be characterized by a boundary layer flow which can be either laminar or turbulent depending on the Reynold number. The boundary layer flow at the bottom and top of the tank accelerate radially outwards due to the centrifugal forces. The boundary layer motion causes a secondary flow to build up in the main flow. [8]

This secondary flow is called Ekman pumping and characterized by the Ekman number

$$E = \frac{\nu}{\Omega \cdot c^2} \tag{1}$$

ν denotes the viscosity, Ω is the rotational velocity and c is the half-height of the tank. The Ekman number can be seen as the ratio of viscous forces against Coriolis forces. As long as $E << 1$ the secondary flow causes the angular momentum

transport from the outer walls inwards be dominated by convection rather than diffusion. Already at relatively high Ekman numbers as studied in this report the Ekman pumping is not just a part of the flow development but the dominating factor to a solid body rotation.

The Ekman pumping is visualized in figure 2 below

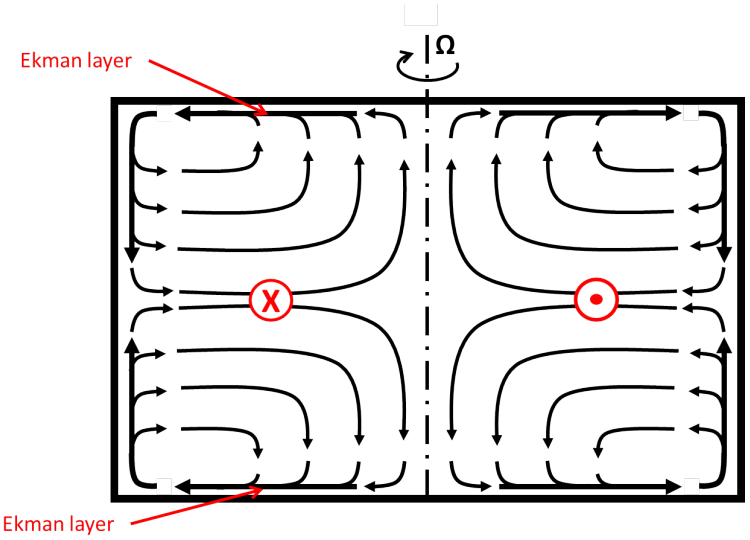

Figure 2: The Ekman pumping developing during spin-up in a full tank.

Figure 2 shows the Ekman pumping building up as the tank is spinning up. The rotational speed of the walls determines the velocity of the boundary layer that is causing the Ekman pumping.

The Ekman pumping is several order of magnitudes slower than the angular velocity of the main flow but it has a dominating effect on the flow buildup. The radial velocity component of the secondary flow causes a transport of the angular velocity from the walls to the center of the tank. This convective transport is shown to be considerable quicker than the diffusive transport and leads to faster buildup of the flow. [8]

At spin-up there are two main forces influencing the flow development, the centrifugal forces and the pressure gradient in the radial direction. At rest these two forces are zero. As the tank starts to spin the flow is exposed to a growing centrifugal force. This force is eventually equaled out by the the pressure. The relationship can be formulated as

$$-\frac{1}{\rho}\frac{\partial p}{\partial n} = \frac{v^2}{r} \tag{2}$$

ρ denotes the density and p the pressure. As long as these two forces are not equal no SBR is reached.

At a solid body rotation the flow has only a angular velocity component. The flow at the outer wall has the same speed as the walls and the velocity is zero in the center of the cylinder. In between these to points the velocity profile develops linearly. Even though small instabilities can form both in experiments as in the numerics, these instabilities have to die out eventually due to dissipation. This is also confirmed by experiments [7]. Thus the linear velocity profile is chosen as a SBR criteria.

2.1.2 Half filled tank

The flow build up for a half filled cylinder is similar to the full tank case. The free surface of the fluid creates additional phenomenas that influences the flow development. The case has less mass to spin-up but it also has less contact area where the momentum from the wall can be transferred to the fluid. Because the top wall is not in contact with the water there will only be one Ekman boundary layer getting its energy from the bottom wall. This is illustrated in figure 3 below

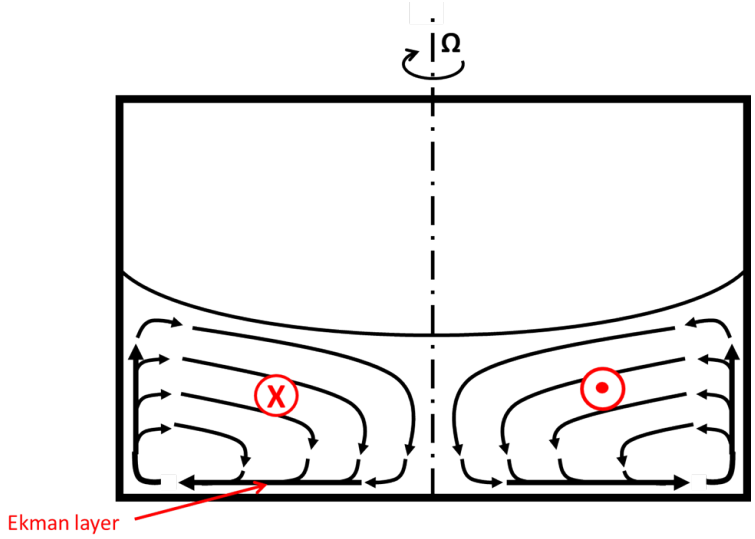

Figure 3: The Ekman pumping developing during spin-up in a half full tank.

Figure 3 shows the one Ekman boundary layer developing at the bottom wall. The parabolic shape of the free surface developing can also be seen. This shape develops due to the changing pressure gradient trying to equal out the centrifugal forces of the flow according to equation 2.

The surface shape influences the direction of the secondary flow i.e. the convective angular momentum transport. Additionally the free surface is interacting with the free surface. This leads to a less powerful secondary flow due to interaction with the free surface. This influences the angular momentum transport caused by the Ekman pumping and therefore the spin-up time.
Secondly the flow movement is no longer restricted by an upper wall. This leads to instabilities and oscillating flows can easier develop and be maintained. Despite all these additional phenomenas the flow should reach a SBR as in the full tank case after a long enough time. All instabilities occurring during the spin-up should die out due to dissipation.
The cases are studied from rest to a solid body rotation. The time it takes for the flow to develop to a SBR is used to compare numerical results to experimental. Some appropriate parameters are chosen to indicate a SBR.

Experimental the flow is visualized with a PIV method by using bubbles as seeding particles in the full tank case [7]. The method allows to measure the time until a linear velocity profile horizontally trough the tank i.e a SBR is reached.

For the half filled tank a second criteria is formulated to validate the computed solutions. The theory states that the centripetal forces are equaled out by the pressure gradient as the SBR is reached, see equation 2. In the half filled tank case this is visualized by the free surface parabola developing. This gives the following SBR criteria. When the parabola shape stops developing a SBR is reached.

2.2 Mathematical models

To run an experiment under the real conditions for the problem formulated in this report is too expensive and not possible today. Therefore simplified experiments are conducted on ground condition. These experiments are always limited by the equipment and budget for the experimental setup.

Another approach is to model the experiments numerically. That brings a greater freedom on the setup and the physical properties. The validation of more complex numerical models keeps on developing and this project investigates the possibility to model highly rotational flows with complex physical models such as a free surface.

Making use of simulations for space application is a growing field of research and has to be validated thoroughly. This is why a lot of effort is going in to model fluids in more complex problems such as in micro-gravity conditions. One of the issues with modeling fluids in space conditions is the absence of gravity. When gravity no longer is the dominant force acting on a flow, smaller forces such as surface tension and adhesion forces need to be modeled. There exits only very limited experimental data to validate these problems today.

An additional limitation for all CFD simulations today is the computer power. This limits the number of cells that can be computed. One effective way of minimizing the cell count is to simulate only 2D geometries or approximate 3D geometries as 2D. It is already known for this case that there are secondary flows occurring. This secondary flows can't be captured in a 2D model. The importance of these secondary flows can easily be shown by computing the case in 2D and comparing the spin-up times with the 3D case. It is shown that the 2D spin-up time becomes much longer than for the 3D case [8]. More about the computation effort for this a 3D case is discussed in section 4.
The CFD solvers are based on several mathematical models that are discussed in this section. Thereafter a detailed description of the solvers setup is given.

2.2.1 Governing equations

The motion of a flow is determined by the laws of physics. The mass conservations law, Newtons second law and the first law of thermodynamics build up the governing equation for a flow. Mass conservation simply states that for a closed system the mass most be constant over time. For an compressible fluid this can be written as

$$\frac{\partial \rho}{\partial t} + \bigtriangledown \cdot (\rho \vec{V}) = 0 \tag{3}$$

ρ denotes is the density, $\vec{V}$ the velocity vectors.
Newton second law states that the force is equal to the mass times acceleration. In a conserved form the compressible momentum equation can be written as

$$\rho \frac{D\vec{V}}{Dt} = \rho \vec{f} - \bigtriangledown p + \bigtriangledown \cdot \tau \tag{4}$$

$\frac{D}{Dt}$ denotes the substantial derivative, τ denotes the shear stresses and f is the force.

The compressible energy equation is given by

$$\rho\frac{De}{DT} = \rho\dot{q} + \bigtriangledown \cdot (k \bigtriangledown \cdot T) + \tau(\bigtriangledown \cdot \vec{V}) - p(\bigtriangledown \cdot \vec{V}) \tag{5}$$

where $\dot{q}$ denotes the source term due to radiation heat transfer.

2.2.2 Time discretization

The governing equations need to be discretized in order to numerically iterate the equations until a solution is found. The case is treated as a transient one which means that it is discretized both spatiality and in time. In order to get physical solutions it is important that these discretization are made fine enough. The mesh controls the spatial discretization and is therefore always a compromise between accuracy and computation time. The time discretization is controlled by the CFL condition which gives the following condition on the Courant number

$$C = \frac{\Delta t \cdot u}{\Delta x} \tag{6}$$

C is the Courant number, Δt denotes the time step and Δx the size of one cell size. The explicit CFL criteria is that $C \leq 1$ which makes sure that the time step is not chosen too large. If the Courant number is greater than 1 the risk is that flow information is missed and cells are skipped during the iterations.

For an implicit time schemes it is possible to break this limit and still capture all the flow information. The time integration scheme used by FINE/Open is the 4th order Runge-Kutta method. This method is explained more in section 6. This makes it possible to have a Courant number up to 3 without getting unstable computations.

2.2.3 Spin-up time

As discussed before, the secondary flow developing during spin-up is dominating the spin-up time already at low Reynolds numbers. Therefore some research has gone in to understanding and model the secondary flow in order to get an analytical formulation for the spin-up time.

According to Thiriot [9] the Ekman layer accelerates for a period of roughly $2/\Omega$ s. After that the boundary layer is considered steady. According to Hyun & Park [1992] [10] the Ekman boundary layer thickness scales with $\sqrt{E}$.

Wedemeyer [8] formulates a set of non-linear differential equations for the spin-up of a cylindrical tank. He starts by formulating the axisymmetric Navier-Stokes equations. He divides the flow development into the core flow and the boundary layer flow. Due to the short acceleration time of the boundary layer stated by Thiriot [9], the boundary layer is approximated by a quasi-steady flow. This makes it possible to find a relation between the boundary layer flow and the core flow by balancing the mass transportation.

Greenspan [11] has extended Wedemeyers work to include spin-up from an arbitrary rotation Ω. He derived a theoretical spin-up time as

$$t_s = \frac{\frac{2c}{a}\sqrt{Re}}{\Omega} \tag{7}$$

where the half height has been taken as the characteristic length. The reason to chose the half-height as the characteristic length is that the Ekman vortexes

seen in figure 2 are mainly limited by the half-height. If the radius is smaller than the half-height, the radius should be taken as the length scale instead. Re denotes the Reynolds number that is define as

$$Re = \frac{R^2 \cdot \Omega}{\nu} \tag{8}$$

R denotes the radius of the cylinder.

Both Weidman [12] and Sedney [13] derive solutions for the spin-up time based on the work of Wedemeyer and get the same solution as Greenspan. The only disagreement in their results is the constant multiplying with to get the real spin-up time. Weidman uses the constant 1/0.443 derived by Wedemeyer whilst Sedney writes down a rule of thumb as

$$t = 4 \cdot t_s = 4 \cdot \frac{\frac{2c}{a}\sqrt{Re}}{\Omega} \tag{9}$$

As the Ekman layer becomes turbulent a turbulent spin-up time scale is derived by Sedney as

$$t_{st} = \frac{28.6 \cdot c}{\Omega \cdot a} Re^{\frac{1}{5}} \tag{10}$$

The limitation of the laminar theory is given around $Re = 10^5 - 10^6$. There are different values given in literature, Wedemeyer had a limit of $Re \leq 3 \cdot 10^5$ but showed experimental data of $Re = 6 \cdot 10^5$, Sedney wrote a limit of $Re \leq 1 \cdot 10^5$ but numerically used a value of $Re = 2 \cdot 10^6$ to calculate the turbulent boundary layer.

2.2.4 Volume of Fluid method

To model the free surface of the half filled tank case, an additional model has to be adapted to deal with the two fluids with different physical characteristics. Several methods have been developed to handle more than one fluid. Two common methods are the level set method and the volume of fluid method. They both have their advantages and disadvantages. The surface development for the current case is expected to be rather smooth with no surface separation or secondary free surface introduced in the system. Therefore the volume of fluid method is chosen to model the free surface. The volume of fluid method is based on the simple concept of having one additional variable field over the whole domain that denotes what phase is present in a cell[14]. More details about the method are given in section 6.

3 State of research

In recent years several commercial CFD softwares have been analyzed for similar problems as the one in this report.

Munk [6] studied the incompressible THETA version of the DLR TAU CFD software. The case studied is a rotating cylinder filled with water. He looked at the codes capability to predict the flow development during spin up and how well the code could maintain a steady rotational solution.
It is found that the code is able to predict a solid body rotation with a structured grid. When initialized with a SBR the code is able to maintain it for several minutes. He encountered unexpected flows when using an unstructured mesh that couldn't be explained.

Schmitt [5] has used Flow-3D and Ansys fluent to simulate the free surface reorientation occurring upon a gravity step reduction. This phenomena is also known as axial sloshing. A 2D problem formulation was used with the volume of fluid method used to model the free surface of a half filled tank. The fluids studied are water and liquid hydrogen, LH2. The result are compared with drop tower experiments. It was found that the pressure distribution could not be modeled correctly.
One reason was that only one thermal equation is solved by fluent. At the free surface the cells contain both liquid and vapor. The temperature in these cells is density-averaged. This leads to a numerical cooling of the vapor and by using the ideal gas law a reduction of pressure. This limitation of using the volume of fluid method is explained more by Foreest et al [16]. A further limitation was set by the computation power. Three different meshes where studied, 17849, 105886 and 408404 cells, and run on 8 cores. The computations for the finest mesh took over two weeks. This limited the resolution of the free surface that showed to be under resolved compared with experimental results. This lead to a under prediction of the wall angle to the super heated wall.

Flanagan [15] validates the open source software OpenFOAM for the full tank case. The work was done parallel to this project and the setup and geometry is the same. The results show that a mesh grading at the walls is needed to catch the wall flow accurately. For the courser mesh of 60x60x120 with wall refinement oscillations continue to disturb the flow even after a SBR is expected. This was improved be choosing a finer mesh of 120x120x120 where no pronounced oscillations remained. A short study on the Courant number showed that the fluctuation are damped down by decreasing the Courant number to 0.25.

4 Computation effort

A clear limitation of any CFD computation today is the computation power available. Especially for a full 3D computations the cell count easily becomes too high for any reasonable computation time.

The mesh refinement used is the dominating parameter to determine the necessary computation time. As it is a 3D case each mesh node has 3 coordinates (x,y,z) additionally the cell size controls the time step via the CFL condition. This leads to a theoretical relationship between the computation time and the number of nodes of an order 4. This relationship makes it desirably to use the coarsest mesh possible to resolve the flow with no unnecessary refinements.

In this section a short investigation of the computation power needed for the cases studied is performed. The data is based on real simulations computed with FINE/Open and DrNUM. The meshes used in this report are listed in table 1.

Case	Mesh resolution	Nr. of cell	$\triangle$x(m)	Aspect ratio
Full Tank FINE	60x60x40	144000	0.005	1
Full Tank DrNUM	60x60x40	144000	0.005	1
Full Tank DrNUM	80x80x55	352000	0.00375	1.03
Full Tank DrNUM	100x100x70	700000	0.003	1.05
Full Tank DrNUM	120x120x80	1152000	0.0025	1
Open Tank FINE	60x60x120	432000	0.0025	3

Table 1: Meshes used in this project.

The meshes are also shown later on in section 5. For the computations with DrNUM a real mesh refinement study is performed and is shown in the results. In order to make the full tank meshes as comparable as possible the aspect ratios is held close to 1. Due to performance issues of FINE/Open only the two meshes shown in table 1 could be tested. The performance issues had nothing to do with the software itself but how the software was setup for the computer cluster used. The initial setup up of the software made for a very poor parallelization performance. A lot of time was spent on improving the grade of parallelization. This was finally accomplished by changing the way of communication between the cluster nodes.

As already mentioned in the introduction, two different CFD softwares are used, FINE/Open that is run on classical CPUs and DrNUM that is run on one GPU. In order to run a CFD software on a GPU the software has to be coded in such a way to fit the simple mathematical operators available on a GPU. A badly coded software can actually run slower on a GPU compared to a CPU. In general however a GPU is much faster than a CPU, often more than a 100 times faster.

To get a clear understanding on the performance difference of a CPU and a GPU the computation time needed for the different meshes are tabulated below.

CFD software	Computation power		Mesh					
500s simulation			2D		3D			
yy:dd:hh	Nr of nodes	Processors	60x60 3600 cells	120x120 14400 cells	60x60x40 116960 cells	100x100x70 847000	120x120x80 1152000	240x240x160 9216000 cells
FINE/Open	1	12 CPUs	0:6:6	0:10:9	0:31:6	-	0:186:16	3:335:8
	2	24 CPUs	0:3:10	0:5:17	0:17:5	-	0:103:1	2:59:13
	6	72 CPUs	0:1:10	0:2:8	0:7:2	-	0:42:10	0:325:5
	12	144 CPUs	0:0:20	0:1:10	0:4:6	-	0:25:9	0:194:14
DrNUM	-	1 GPU	-	-	0:0:7	0:2:18	0:5:4	0:70:5
	-	10GPUs	-	-	0:0:1	0:0:7	0:0:12	0:7:0

Table 2: The computation time yy:dd:hh for different meshes.

Table 2 shows the computation times required for different meshes. The time format is shown in yy:dd:hh. From table 2 it becomes clear that with todays CPUs extremely large computer clusters are needed to get a reasonable computation time for larger computations. An example is the 240x240x160 mesh on the far left in table 2. It will take 144 CPUs 194 days to simulate the problem for 500s. In comparison 10 GPU will perform the same computation in 7 days. This makes the computation power of a GPU far greater than a CPUs. It should be mentioned that a GPU is more expensive than a CPU. But the price difference does not outweigh the difference in performance.

One more important aspect is that running a CFD code on a GPU in this way is fairly new. This means that there are not a lot of CFD softwares that are able to run on GPUs today. The ones that are able to, like DrNUM are in the development stage and are therefore lacking a lot of the more complex physics that commercial softwares have built in today. One limit of the DrNUM softwares that becomes clear in this report is the lack of model free surfaces i.e. the half filled tank case. This is under development and in a couple of years the variety and complexity of GPU run CFD codes will have developed further.

5 Setup

The results are divided in two parts. In the first part the full tank is studied i.e. the tank is full of water. In the second half a multi phased flow is studied i.e. the tank is half full of water and the other half is air. The full tank is filled up with water all the way to the top and no air or other secondary liquids are in the tank. The physics behind such a case are explained in the theory section. The half filled tank is half filled with water, the water level at rest is at 0.1m. The geometry of the tank can be seen in figure 1. The geometry is chosen to fit experiments that are conducted parallel to this work by master student Jakob Svensson [7].

The setup of the simulations is simplified as much as possible. The tank is initially at rest with no velocity component in the flow. The cylinder walls are instantly set to a fix rotation. The rotation speeds studied in this report are 30 RPM, 60RPM and 90RPM. These rotation speed are chosen to match the experiments conducted. The fluid studied is water which corresponds to Reynolds numbers of 71000, 141000 and 212000. A short table of the physical properties is shown below

Case physics	Real condition	Modeled condition
Body forces	Micro-gravity	Full gravity
Temperature	Cryogenic conditions	300K
Flow velocity	$Re \approx 1250000$	Re 71000-212000
Fluid	Liquid hydrogen	Water
Initial condition	Not necessarily at rest	Rest
Forces	Rotational and lateral	Only rotational
Wall temperature	Heated walls	Isothermal
Tank	Complex geometry	Simple cylinder

Table 3: Simplification of the problem.

Table 3 highlights the simplifications made for this case. Many of these simplifications are made to fit the experiments in order to validate the results.

Full gravity and a temperature of 300K is imposed in order to model the ground conditions of the experiment. The motor used for the experiments limits the rotational speed. Because water is desirable to use for the experiments it also limits the Reynold numbers reached. The case is set up as isothermal i.e. no energy equation is solved. In the physical experiments this is not the case. However the temperature exchange between fluid and tank walls is considered negligible.

5.1 Full tank

The flow expected for the full tank case is explained in section 2.1.1. In order to get good benchmark values to validate and compare the CFD softwares uniform meshes are chosen.

5.1.1 FINE/Open with OpenLabs

For the full tank a unstructured uniform cartesian mesh is chosen as an initial mesh. The mesh is generated in FINE/Open mesh generator HEXPRESS. The mesh resolution is 60x60x40 and was limited by the performance of the software setup.

The mesh generated in HEXPRESS can be seen in figure 4 below.

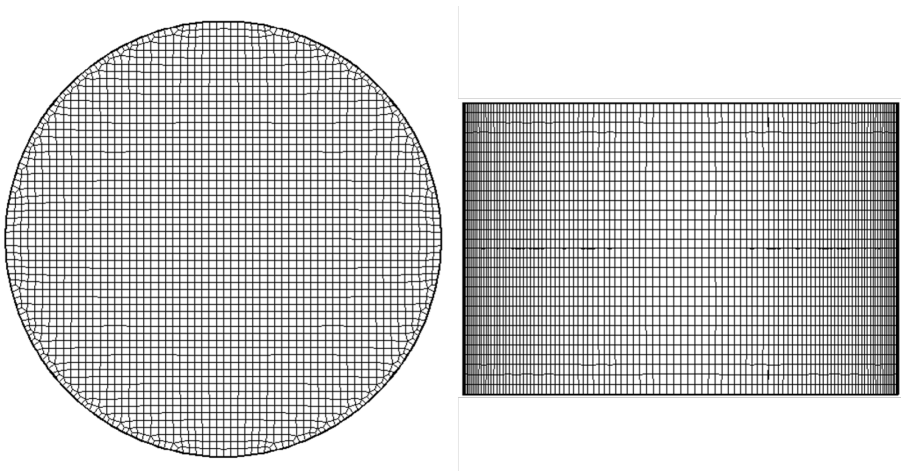

Figure 4: The 60x60x40 mesh used for the full tank case.

The mesh resolution is chosen to get an aspect ratio of 1. This is the only mesh tested for this setup. The reason for this becomes clear from table 2. To compute a simulation with this mesh for 500 seconds would take 1 node roughly 31 days, which is too long for this kind of study. As the grade of parallelization of the software got better it took roughly 4 days on 12 nodes for each simulation. Because of that no mesh refinement study was performed. This means that the results need to be considered with care.

5.1.2 DrNUM

DrNUM does not have a free surface model yet. Because of this limitation only the full tank is computed. The meshes created for this case are described in table 1. The meshing process for DrNUM is further described in section 6.2. The greater computation power of the GPU makes it possible to perform a mesh refinement study. This refinement study is performed for the highest RPM studied i.e. 90 RPM and shown in the results. If a mesh is able to catch all the velocity gradients properly for the 90 RPM case it should also catch lower velocities such as the 30RPM and 60RPM case.

5.2 Half filled tank

The half filled tank case requires a mesh refinement in order to catch the characteristics of the free surface between the two phases. This is a clear requirement of the volume of fluid method. The volume of fluid method is explained in the section 6.1.6. One of the main challenges with this method is to accurately capture the free surface. In order to do that the surface need to be resolved with at least 3-4 mesh layers. [17] The final grid chosen is a 60x60x120 grid. The mesh can be seen in figure 5 below.

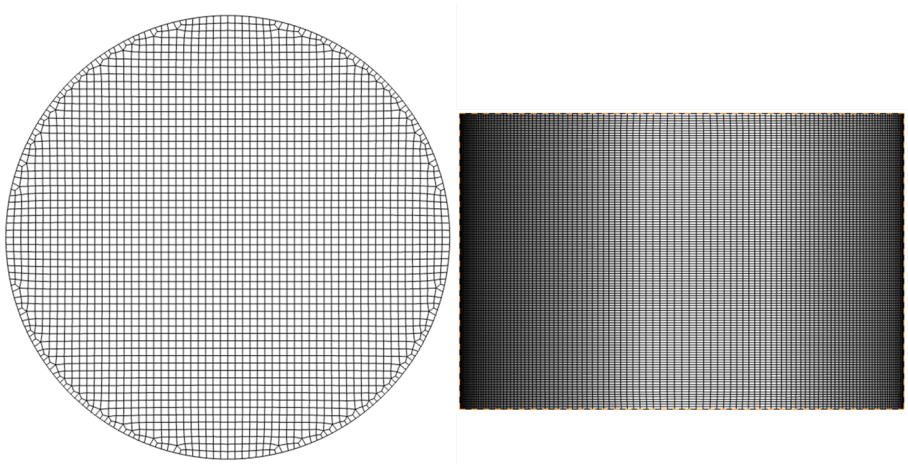

Figure 5: The 60x60x120 mesh used for the half filled tank case.

From the figure it can be seen that the cells are much finer in the z-direction than before. The reason for this is to better catch the free surface that initially is at rest. The setup at rest is shown in figure 6 below

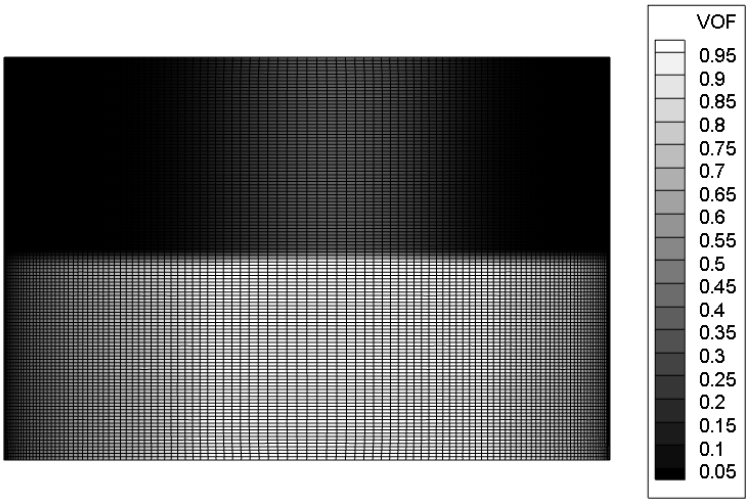

Figure 6: Visualization of the half filled tank at rest.

Figure 6 shows the water at rest. The water is represented by white and the air by black. Some simpler meshes are tested as well. Due to the poor performance they are not shown here. The performance is shown and discussed in the results.

5.3 Validation

In order to compare and validate the simulations against the conducted experiments some appropriate flow parameters are chosen. As discussed in section 2.1 the velocity profile of the flow should go to a linear profile which is a good validation point. The velocity profiles in the results are taken horizontally trough the center of the tank. The linear profile is visualized in figure 7.

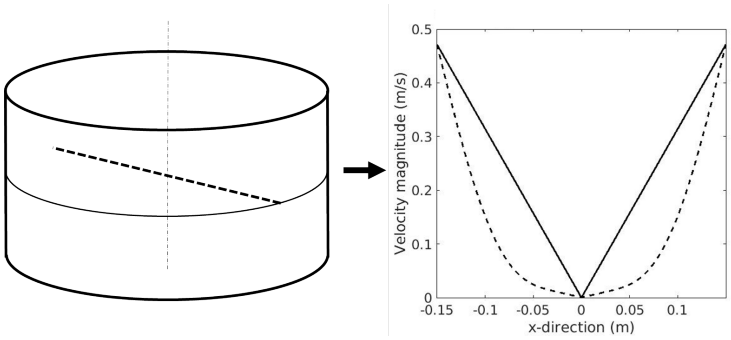

Figure 7: The velocity probe line is shown in the center of the tank.

In figure 7 the velocity profile is shown to the right. The plot to the right has the x-coordinates of the tank on the x-axis and the velocity magnitude on the y-axis. The solid line denotes the theoretical linear profile which the velocity shown as a doted line should reach as the flow gets close to a SBR.

With FINE/Open there was a velocity jump occurring at the walls of the cylinder. This error has been adjusted in the results by matching the theoretical velocity profile to the hight of the velocity jump. The results with this method are denoted as Fine adjusted in the result section.

To get a good comparison between the different simulations a parameter named the evolution criteria is calculated as well. The evolution criteria indicates how close the velocity profile is to a fully linear profile.

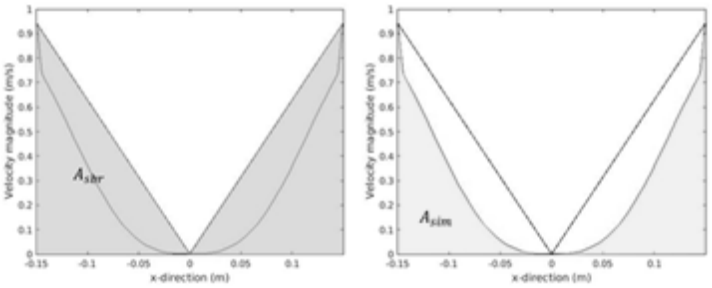

Figure 8: The evolution criteria calculation visualized.

The evolution criteria is calculated as

$$\lambda = 100 \cdot \frac{A_{sim}}{A_{sbr}} \tag{11}$$

where A_{sim} denotes the area under the simulated velocity profile, A_{sbr} the area under the theoretical linear velocity profile and λ the evolution criterion. From this evolution criteria a SBR criteria is set. The spin-up time is taken when the simulated velocity reaches 95% of the linear velocity profile i.e $\lambda = 95$.

The additional validation step for the half full tank is to look at the free surface development. As described in the theory section the parabola height should stop developing once a SBR is reached. This is measured by monitoring the development of the parabola height visualized in figure 9.

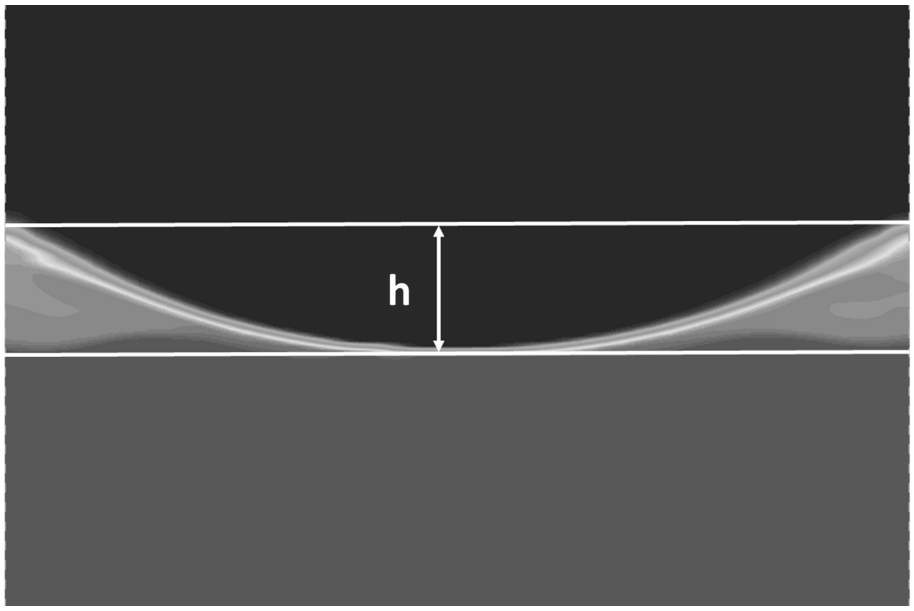

Figure 9: The parabola height measurement.

The parabola height is measured as the distance between the highest and lowest cell with a VOF fraction of 0.5 which is the mean value between water and air. The SBR criteria for h is the following. When h stops increasing a SBR is said to be reached.

6 CFD solvers

In this report two numerical solver are used to solve the rotating cylinder flow. The first and main solver used is one of Numecas CFD softwares, FINE/Open with OpenLabs. FINE/Open with OpenLabs is used as an incompressible solver with a hexahedral mesh. It contains a combination of advanced preconditioning and a multi-grid acceleration and adaption techniques.

The result are compared with enGits CFD software DrNUM. DrNUM is run on a GPU, graphics processing unit. It uses a dual resolution mesh that is further explained in section 6.2 [4].

The advantage of running on a GPU is that GPUs require a fraction of the computation time compared to a standard CPU. This gives the opportunity to run computations with a much finer mesh than what is possible on an CPU for the same computation time.

DrNUM has the limitation that it does not have a free surface solver yet. Because of that only the full tank case is compared between the two softwares.

To understand the numerical part of the CFD solvers is very important to understand and validate the results. Therefore the numerics used by each software are explained in more detail in the next sections. As DrNUM is under development there doesn't exist that much documentation about it yet.

6.1 FINE/Open

FINE/Open with OpenLabs is an commercial CFD solver provided by Numeca. It can solve both incompressible and high speed flows. It uses a fully hexahedral unstructured mesh with an coarse grid initialization. OpenLabs allows the user to change all of the physical and numerical models. [17]

6.1.1 Physical configuration

Due to the physical flow behaviors described in section 2.1 and the desire to get a spin-up time the problem is computed as an unsteady case. Some early test simulations showed that the flow stays laminar for the spin-up except for the first seconds of acceleration. Therefore the laminar Navier-stokes equation is used as the flow model. Due to the low Reynolds numbers the fluid was modeled as incompressible.

6.1.2 Boundary conditions

The boundary conditions are set to simple Dirichlet conditions with a constant rotation speed. All three walls have the same rotation speed. The cylinder walls are set as adiabatic i.e. no energy equation is solved.

6.1.3 Initial solution

The initial solution for all the cases in this report is no rotational velocity at t=0, the fluid is at rest before spin-up. The initial solution is computed by a coarse grid initialization. The coarse grid initialization starts the computation by iterating over a very coarse mesh. Ones a solution is converged on that grid level it is interpolated to the next finer grid. This process is continued until the finest grid is reached. The effect of the coarse grid initialization is that the multiple grid refinements damps out low frequency errors.[17]

6.1.4 Numerical parameters

The spatial discretization of the Navier-Stokes equation is based on a cell centered finite volume approach and performed by a second order central scheme.[17]
The second order central scheme is formulated as

$$\frac{\partial \phi}{\partial x} = \frac{\phi_{i-1,j} - \phi_{i+1,j}}{2 \triangle x} + \mathcal{O}(\triangle x^2) \tag{12}$$

The cell centered finite volume methods computes the flow variables in the center of the control volume as an average over the grid cell.[18]

The time discretization is based on a dual-time stepping technique and performed by a 4th order Runge-Kutta scheme. The 4th order Runge-Kutta scheme is written as

$$\begin{aligned} \frac{\partial U}{\partial t} &= F(U) \\ U^1 &= U^n + \alpha_1 \triangle t F(U^n) \\ U^2 &= U^n + \alpha_2 \triangle t F(U^1) \\ U^3 &= U^n + \alpha_3 \triangle t F(U^2) \\ U^4 &= U^n + \alpha_4 \triangle t F(U^3) \\ U^{n+1} &= U^4 \end{aligned} \tag{13}$$

where U^n denotes U at t and U^{n+1} U at $t + \triangle t$. The coefficients α are set to

$$\alpha = (0.25, 0.33, 0.5, 1) \tag{14}$$

this is the standard configuration of the Runge-Kutta method used by the software. [17]

The dual-time stepping technique is based on taking larger implicit time steps with a large stability region and solve the implicit equations at each time step with a couple of inner iterations. [19] The number of inner iterations needs to be set large enough, 50 steps are used, in order to get a good convergence.

A precondition method developed by Hakimi [20] is used to increase the efficiency of the time stepping. The lack of efficiency at low speeds is due to a high disparity between the convective and acoustic eigenvalues. This makes the time steps too restrictive which leads to poor convergence characteristics.

6.1.5 Computation control

The computations performed are simulated for a total physical time of 500s. This value is based in early experiments that show that the solid body rotation is captured in that time span.

According to recommendations from Numeca the physical time step is set to 50ms which responds to roughly $\frac{1}{20}$ of the flow frequency expected. [17]

The computations are performed with a multi-grid method in order to get a fast convergence and damp out any low frequency errors. There are different multi-grid strategies that can be used to make sure that all the frequencies are damped out.

The simplest strategy is the V-cycle method which is used for the computations in this report. The strategy of the V-cycle id visualized in figure 10 below

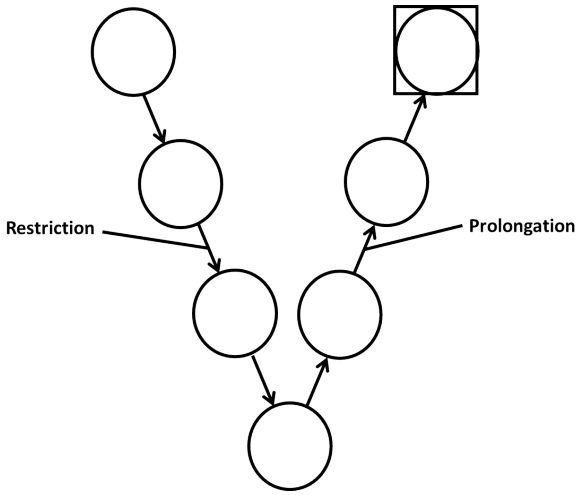

Figure 10: Visulaisation of a multi-grid V-cycle strategy.

The method consist of four restrictions from the finest to the coarsest mesh and then back to the final solution marked with a square. [17]

6.1.6 Volume of Fluid Method

For the half filled tank case a free surface model is used to model the surface of the water. The Volume of Fluid Method is a numerical method developed to model the interface between two phases. The model was introduced 1976. The two fluids have to be immiscible incompressible and isothermal in order for the method to work. [14]

The concept is to introduce an additional scalar field that denotes the different phases. This scalar field is the VOF fraction, it keeps track on what phase is included in the calculations.

The VOF fraction defines the average density and dynamic viscosity as:

$$\rho = C\rho_1 + (1 - C)\rho_2 \tag{15}$$

$$\mu = C\mu_1 + (1 - C)\mu_2 \tag{16}$$

here C denotes the VOF fraction, μ the dynamic viscosity and he subscripts 1,2 denote the two different phases. [14]

The cells at the free surface that contain both air and water will according to these equations get a mean value of density and viscosity of water and air. The method is visualized in figure 11 below

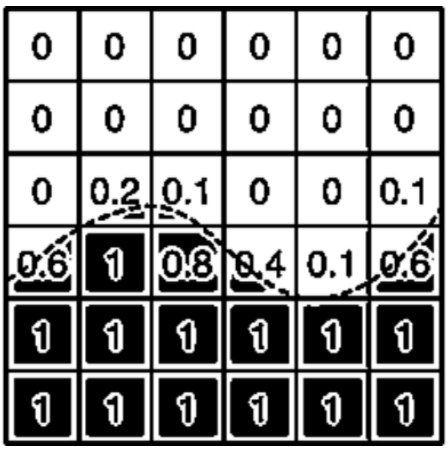

Figure 11: Visulaisation of the mass fraction with the volume of fluid method.

In figure 11, 1 denotes water, 0 denotes air and at the surface it becomes a mean value of the two.

In reality this is of course not the case. In reality the phase change is a sharp boundary but this is very hard to model numerically. This is why the resolution at the free surface has to be fine, so that the phase change gets as sharp as possible.

6.2 DrNum

DrNUM is a new CFD software that is being developed by enGits GmbH and numrax GmbH and was released in 2013. The case in this report needs to be modeled in 3D to capture the most important flow development. To model in 3D very quickly leads to a high number of cells in order to get a decent mesh resolution. This makes the computation time for a computation needed a clear limitation on the simulations. DrNUM provides a good opportunity to have a mesh resolution within a reasonable computation time.

DrNUM uses a dual resolution mesh that consist of so called patches. These patches make up a coarse mesh of super-nodes. These super-nodes can overlap and each one consist of a much finer mesh which is the mesh that the numerical calculations are based on. [4]

7 Results

7.1 Full tank

For the filled tank the simulations are validated by the velocity profile horizontally through the middle of the tank described in section 5.2.1. The velocity profiles are shown at 100s, 200s and 500s simulated with both FINE/Openlabs an DrNUM. Afterwards the evolution criteria and the spin-up times are compared.

Because if its dominating effect on the spin-up time the modeling of the Ekman pumping is shown as well.

7.1.1 FINE/Open with OpenLabs

The results for the full tank computed with FINE/Open with OpenLabs are shown below. The rotation speed studied are 30RPM, 60RPM and 90RPM.

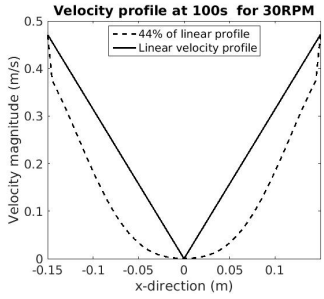

a) 30RPM @ 100s

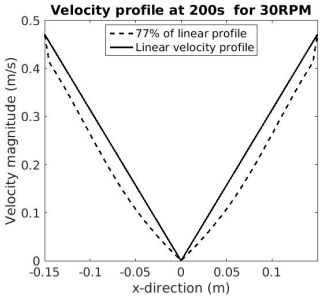

b) 30RPM @ 200s

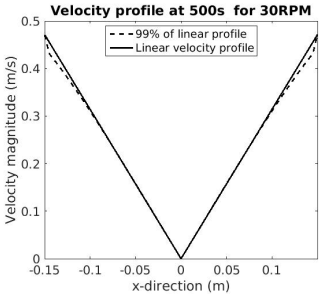

c) 30RPM @ 500s

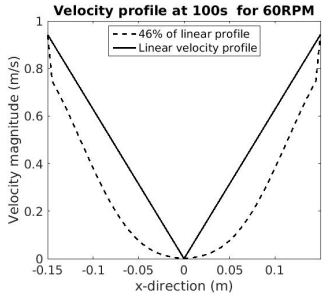

d) 60RPM @ 100s

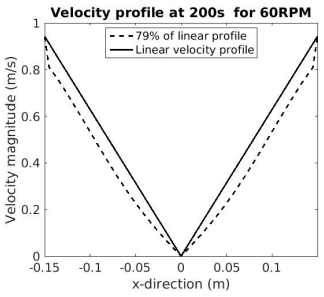

e) 60RPM @ 200s

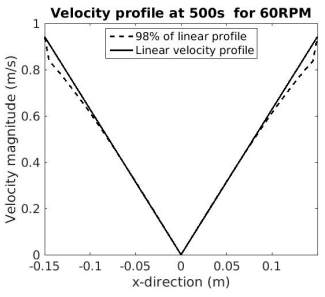

f) 60RPM @ 500s

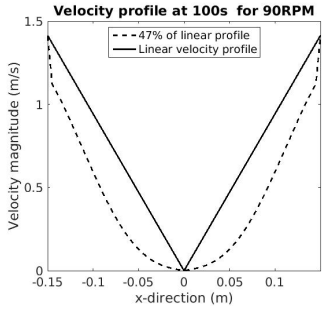

g) 90RPM @ 100s

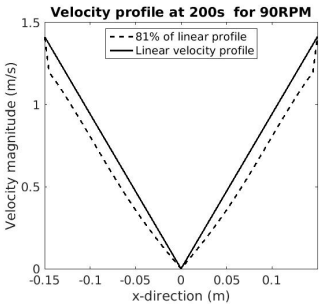

h) 90RPM @ 200s

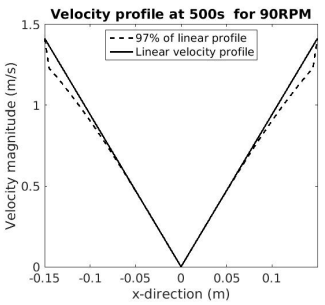

i) 90RPM @ 500s

Figure 12: The velocity profiles simulated by FINE/Open with OpenLabs for the full tank.

Figure 12 shows the velocity profiles simulated from the different rotation velocities. It can be seen that for all rotational speeds the velocity profile is converging towards the linear shape of a SBR. However a small error can be seen at the outer wall of the cylinder where the simulated velocity has a clear jump in velocity for all three rotational speed. This error seems to grow with rotational speed. A closer investigation of this velocity jump showed that it occurs at the first mesh layer. This error is more discussed in section 8.

As discussed in section 2.1 the effect of Ekman pumping dominates the spin-up time. It is therefore of interest to see how well the Ekman vortexes are captured numerically, this is shown in figure 13 below

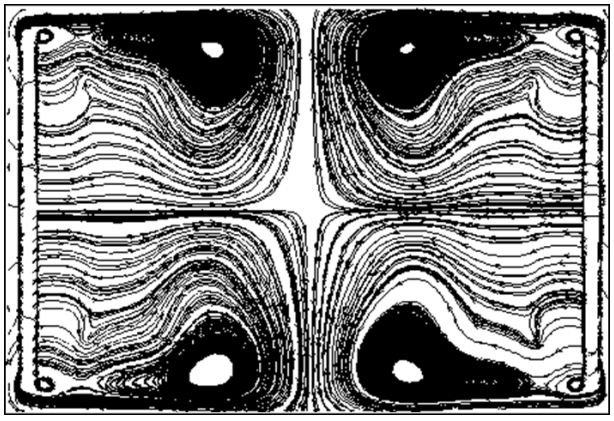

Figure 13: The Ekman pumping developed during spin-up.

From figure 13 it can be seen that FINE/Open captured the Ekman pumping well. This is the case for all three rotational speeds computed.

7.1.2 DrNUM

The results of the grid refinement study performed with DrNUM are shown below.

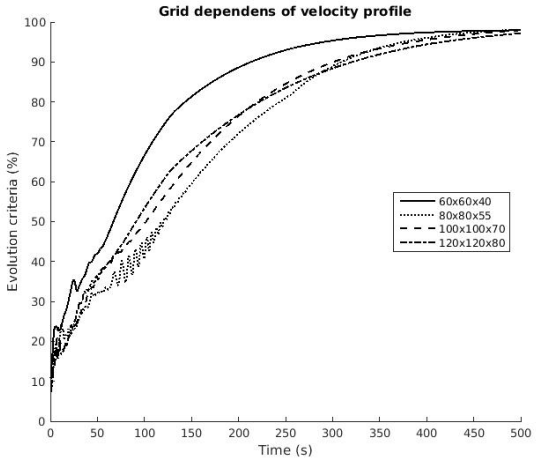

Figure 14: The grid refinement study with DrNUM.

Figure 14 shows the grid refinement study performed with DrNUM. It is visualized by the evolution criteria over time. The results show that the flow for the 60x60x40 mesh reaches a SBR much faster than the other meshes. On the other

hand the 80x80x55 mesh shows the slowest flow convergence of all the tested meshes. Meshes 100x100x70 and 120x120x80 show quite similar results for the evolution criteria. Based on this the 100x100x70 mesh is chosen as the mesh to compute.

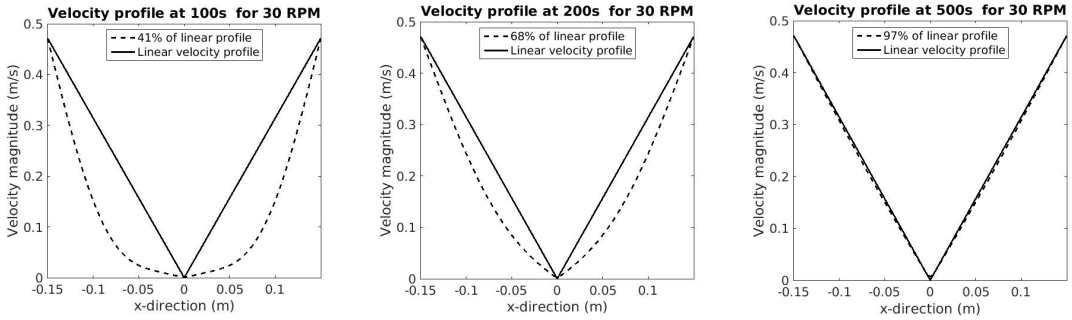

a) 30RPM @ 100s b) 30RPM @ 200s c) 30RPM @ 500s

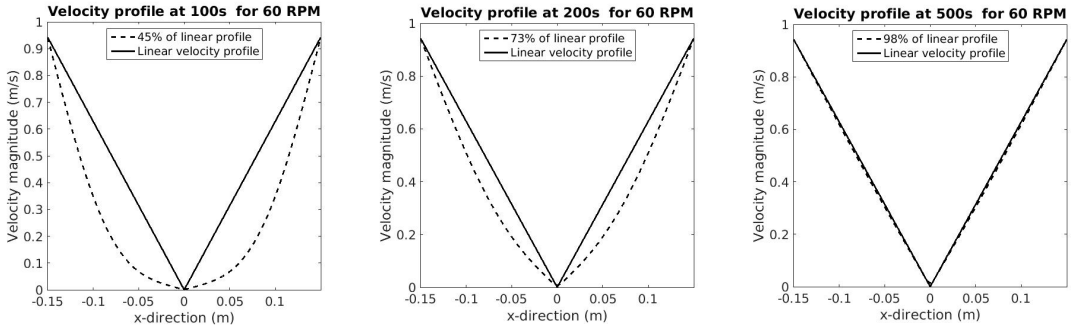

d) 60RPM @ 100s e) 60RPM @ 200s f) 60RPM @ 500s

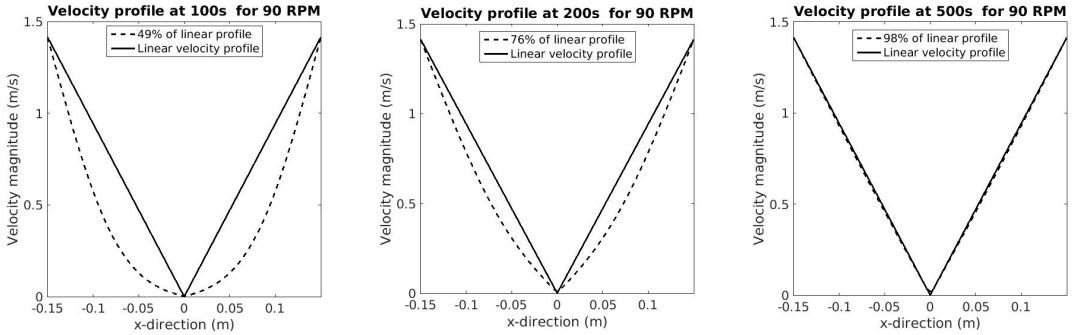

g) 90RPM @ 100s h) 90RPM @ 200s i) 90RPM @ 500s

Figure 15: The velocity profiles simulated with DrNUM for the full tank.

Figure 15 shows the velocity profiles for the rotational 30RPM, 60 RPM and 90RPM computed with DrNUM. The results show that the velocity is converging to a linear velocity profile over time. At 500s the velocity profiles are almost a perfect linear profile as expected. No velocity jump near the wall as for FINE/Open can be seen.

7.2 Full tank comparison

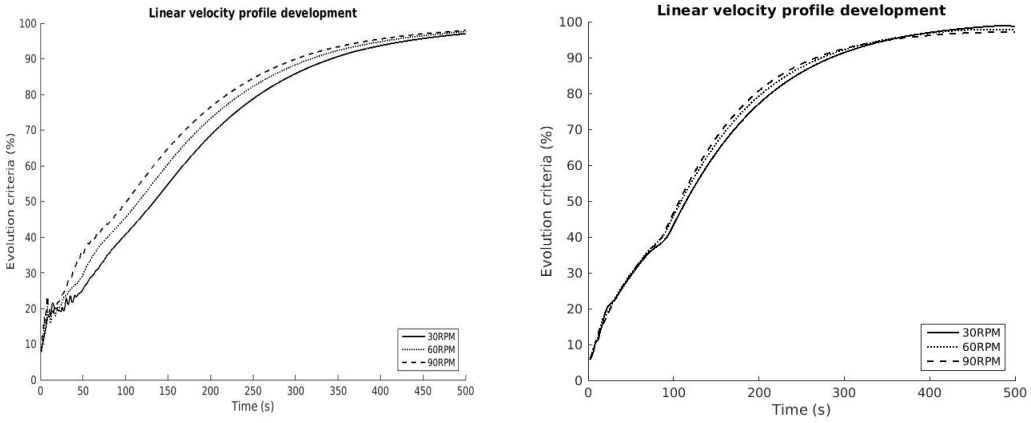

a) DrNUM evolution criteria b) FINE/Open evolution criteria

Figure 16: The evolution criteria plotted against the time for both DrNUM and FINE/Open.

In figure 16 it can be seen that the evolution criteria is converging nicely over 95%. The simulations computed with DrNUM show a larger variance with rotational speed than for the FINE/Open results which don't seem to be vary much with rotational speed. DrNUM seems to capture the trend of an faster spin-up for a higher rotational speed whilst FINE/Open does not.

7.3 Half filled tank

All the results shown in this section are computed with FINE/Open. Early simulations showed instabilities in the free surface. A damping factor was increased to get a stable surface development. According to Numeca the amount of damping used is a good compromise between accuracy and stability.

The velocity profiles for the half filled tank are shown in figure 17 below.

7.3.1 Velocity profiles

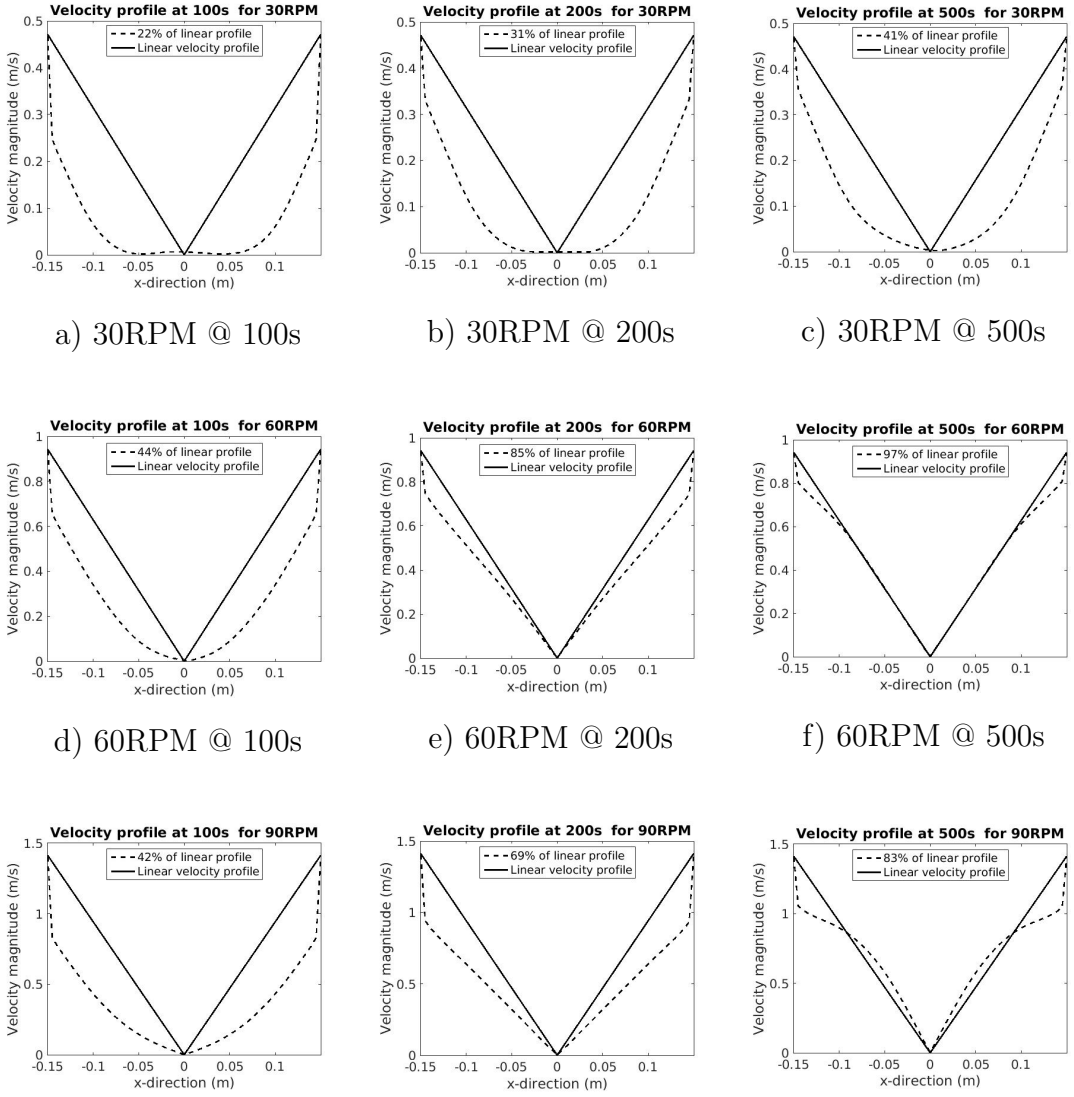

a) 30RPM @ 100s b) 30RPM @ 200s c) 30RPM @ 500s

d) 60RPM @ 100s e) 60RPM @ 200s f) 60RPM @ 500s

g) 90RPM @ 100s h) 90RPM @ 200s i) 90RPM @ 500s

Figure 17: The velocity profiles for the half full tank.

A larger dependence of the rotational speed can be observed. At 30RPM the flow doesn't reach a linear velocity profile even after 500s, seen in 17 c). The velocity jump at the walls that could be observed for the full tank can even be seen here. For 60 RPM it gets close to a linear velocity profile and the wall velocity jump grows larger, can be seen in 17 f). For 90RPM the wall velocity jump is severe. Furthermore the velocity seems to overshoot the linear profile in the middle of the tank. This is a clear physical violation and shows that the computed results can not capture the real flow development fully.

7.3.2 Flow development

Figure 18 below shows how well the Ekman pumping is captured for a half filled tank.

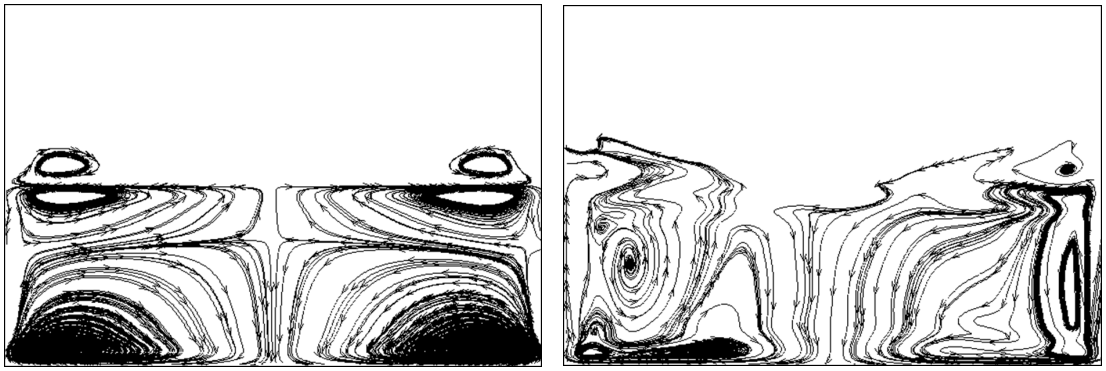

a)Ekman pumping first 10s b) Streamlinens after 10s

Figure 18: The Ekman pumping during spin-up of the half filled tank.

From figure 18 it can be seen that the computation is not able to predict the Ekman pumping in a correct way. Similar results are observed for all the tested rotational speeds.

The evolution criteria of the half filled tank is shown below.

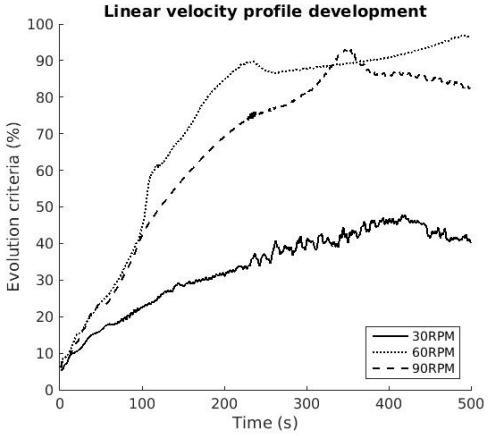

Figure 19: The evolution criteria for the half filled tank.

Figure 19 shows that the flow doesn't converge to a linear velocity profile as smooth as for the full tank case. For 30RPM it doesn't come close to a linear velocity profile even after 500s. For 60RPM and 90RPM it gets up to around 90% but it is not really smooth.

7.3.3 Parabola development

As discussed in section 2.1.2 the parabola development is also a good parameter to show that a SBR is reached. The development of the parabola is shown in figure 20 below

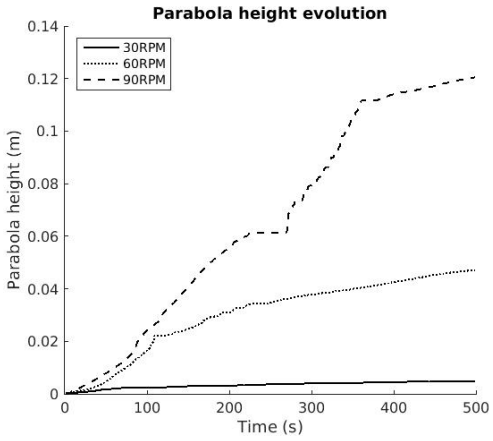

Figure 20: Parabola height development for the half full tank.

Figure 20 confirms that no SBR is reached for the half filled tank. One of the criteria for a SBR is that the parabola height stops developing. It can be seen that after 500s the parabola height for all three rotational speeds keeps on developing i.e. no SBR is reached.

7.3.4 Mass conservation

As the mass conservation is a known issue for any free surface model the volume fraction is plotted against the time in figure 21 below.

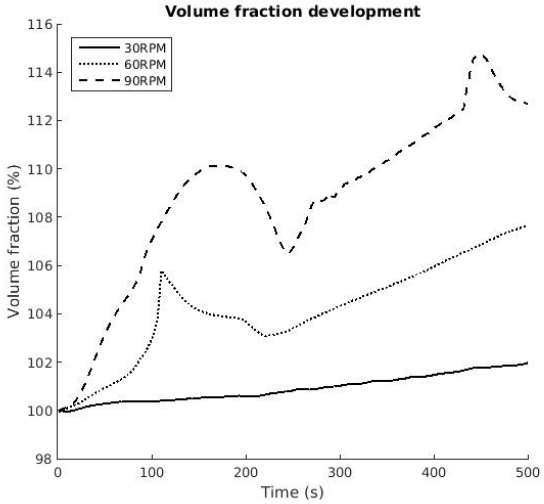

Figure 21: The volume fraction for the half filled tank.

The figure shows that the mass conservation is not held for any of the free surface computations. A summary of the free surface results is tabulated below

Rotational speed	Evolution criteria	Water increase	Parabola height
30RPM	40.10%	2.00%	0.49cm
60RPM	96.70%	7.60%	4.70cm
90RPM	82.60%	12.7%	12.05cm

Table 4: Summary of the free surface computations.

7.4 Comparison to experiments

Parallel to the work presented in this report, experiments on the same setup are performed by master student Jakob Svensson [7]. In this section the numerical results are compared to the experimental. Additionally the theoretical spin up time formulated by Wedemeyer[8] are tested as well. In figure 22 below the spin-up times for the full tank are compared

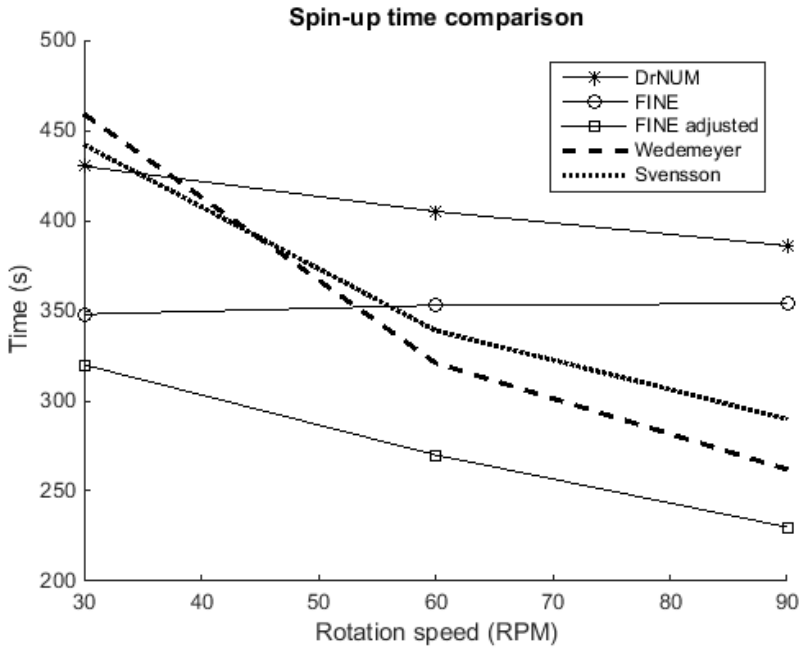

Figure 22: Spin-up time comparison between theory, experiments and numerics

From figure 22 it can be seen that the experimental results from Svensson fit the theory of Wedemeyer quite well. Numerically neither software is able to predict the right spin-up time. The results computed with DrNUM show that the the spin-up time for 30RPM matches the theory well but when going to higher RPM the spin-up time gets much longer than the theory predicts.

Two measurements are shown for the FINE/Open with OpenLabs computations. The "FINE" value is the time it takes the evolution criteria to reach 95% with no adjustment made. These values show all around 350s independent of the rotational speed. This happens due to the velocity jump shown in figure 12. A secondary measurement was taken where the linear velocity profile is adjusted for the velocity jump. The measurements are shown as "FINE adjusted". They show a better dependents on the rotational speed and seem to have a similar slope as the spin-up times 60RPM and 90 RPM measured by Svensson. However for all rotational speeds FINE/Open with OpenLabs seem to underpredict the spin-up by roughly 65s.

It can be concluded that neither DrNUM nor FINE/Open with OpenLabs is able to predict a correct spin-up time with the meshes tested.

For the half filled tank no theory is found to calculate the spin-up time. Svenssons experiments show that no clear dependents on the rotational speed can be found for the spin-up time. The numerical results are not able to reach any real SBR hence no spin-up time can be predicted.

8 Discussion & Further work

The simulation computed with both FINE/Open and DrNUM are able to predict the main characteristics of a flow developing as a cylindrical tank is spinning up from rest. Both softwares are getting close to a linear velocity profile for the full tank case.

The simulations with FINE/Open show a velocity jump near the outer walls. Due to the fact that it always seem to happen after the first mesh layer and that the jump is very discrete it points to a numerical error or a incorrect setup of the boundary conditions. The boundary condition are correct and a no-slip condition is ensured. The fact that it occurs in all simulations computed with FINE/Open, both filled and half filled tank makes a wrong set up more unlikely. This gives the conclusion that there is something in the software code that produces these velocity jumps.

Another aspect that should be considered is that only one mesh is computed for the full tank computations with FINE/Open. The resolution is 60x60x40. The results from the mesh refinement study performed with DrNUM showed that a 60x60x40 mesh is not FINE enough to capture the flow development correctly. This gives the conclusion that if FINE/Open requires the same resolution as DrNUM, the 60x60x40 mesh is not fine enough to really capture the flow development. This is is also shown in the simulation performed by Flanagan [15] who used a wall refinement. As further work a finer mesh should be computed and the results compared to the one in this report.

The problem computed is a close system with a single energy input that comes from the cylinder walls. In order to get a correct flow development this energy exchange between wall and fluid needs to be captured fully. Therefore a grid refinement near all the walls is desirable.

The largest velocity gradient occur at the outer walls and by refining the mesh at the outer walls the time step could possibly be increased while still satisfying the CFL criteria of Courant number=1. This would give a more efficient use of the available computational power.

The mesh refinement at the top and bottom wall is desirable because it is where the Ekman pumping is initialized. The correct capturing of the Ekman pumping leads to a better prediction of the whole flow development and the spin-up time. Overall the achieved results are a good first step but there is a lot more that can be done.

The simulation computed for the half filled tank are not able to predict a SBR even after 500s. One reason for this are the instabilities that develop during spin-up. Due to the free surface the fluids are able to slosh around in the tank which leads a more unstable flow development. Instabilities in the flow can also occur in the real spin-up experiment but are then quickly damped out by the viscous forces. FINE/Open is not able to damp down the upcoming instabilities fast enough. But as for the full tank case this can also be largely to the fact that a not fine enough mesh is used.

The reason why this seemingly easy flow problem is difficult to numerically compute is because it is a closed system. Most computed flows have input and an output. Errors that occur during the flow development will only have a limited chance to grow until they are out of the computed domain. However for a closed system as a rotating cylinder, any error that occurs has the potential to grow and stay in the domain for the entire computation. This has the effect that even the seemingly smallest error can have a deciding effect on the flow development. This makes it very important to model the dissipation of the fluid correctly in order to damp out all errors that might occur.

This report is a first step in investigating the possibility of simulating the fuel sloshing occurring in the upper stage tank of the new Ariane 6 rocket. The results show that under strongly simplified conditions the main characteristics of the flow development are captured. However the spin-up time is not predicted correctly yet. This can be improved by using a finer mesh with an additional wall refinement.

As soon as a free surface is introduced FINE/Open struggles to simulate the correct flow development. The damping of the instabilities occurring during spin-up needs to be investigated more. Secondly the mass conservation of the volume of fluid method needs to be improved.

As there is only one free surface that is expected to develop smoothly during spin-up the possibility of treating the free surface as a boundary condition could be another way forward. However this would only hold for these strongly simplified conditions. In real conditions there a lot of other phenomenons like boiling and evaporating due to the super heated walls of the tank that will occur. This means multiple free surfaces that need to be modeled.

From the results achieved in this project it seems unlikely that the numerical softwares will have developed far enough to model the fuel sloshing under real conditions before Arianes first test flight which is in 2020. However even if it is not possible to model the whole tank yet, it might be possible to model parts of the flow development and draw some valuable insights on the fuel sloshing for the upper stage.

References

[1] www.esa.int, (2005). Testing the new Vinci engine. [online] Available at: *http* : *//www.esa.int/Our_Activities/Space_Transportation/Testing_the_new_Vinci_engine* [Accessed 12 Apr. 2018]

[2] Richard Schwane. European Space Agency. ESTEC, The Netherlands.

[3] www.numeca.com, (2016). FINE/Open with OpenLabs. [online] Available at: http://www.numeca.com/product/fineopen [Accessed 12 Apr. 2018].

[4] www.engits.com, (2013). DrNUM. [online] Available at: http://www.engits.com/drnum—cfd-code.html [Accessed 12 Apr. 2018].

[5] Schmitt, S. (2017). Experimental and Numerical Investigation of Two-Phase Flow with Non-Isothermal Boundary Conditions under Microgravity Conditions. Bremen: CUVILLIER VERLAG.

[6] Munk, J. (2016) Numerishe Untersuchung von rotirenden Flüssigkeiten mit dem DLR THETA code. Technischen Universität München.

[7] Svensson, J. (2018) Experimental Study of Spin-Up of a Fluid-Filled Cylindrical Tank. Lund University, Energy Science.

[8] Wedemeyer, E.H. (1964). The Unsteady Flow Within a Spinning Cylinder. Journal of Fluid Mechanics 20(03):383 - 399, [online], Available at: *https* : *//www.researchgate.net/publication/*231982440*_The_Unsteady_Flow_Within_a_Spinning_Cylinder* [Accessed 12 Apr. 2018]

[9] Thiriot, K.H. (1940) Über die laminare Anlaufströmung einer Flüssigkeit über einem rotierenden Boden bei plötzlicher Änderung des Drehungszustandes. Journal of Applied Mathematics and Mechanics/Zeitschrift für Angewandte Mathematik und Mechanik 20 (1940), pp. 1–13.

[10] Hyun, J.M. Park, J.S. (1990) Spin-up from rest of a compressible fluid in a rapidly rotating cylinder. Journal of Fluid Mechanics 237 (Apr. 1992), pp. 413– 434. ISSN: 1469-7645.

[11] Greenspan, H.P. (1968) THE THEORY OF ROTATING FLUIDS. Cambridge. New York: Cambridge University Press.

[12] Patrick D. Weidman. (1976) On the spin-up and spin-down of a rotating fluid. Part 1. Extending the Wedemeyer model. Journal of Fluid Mechanics, Volume 77, Issue 4, 22 October 1976 , pp. 685-708

[13] Sedney, R. Gerber, N. (1983) OSCILLATIONS OF A LIQUID IN A ROTATING CYLINDER: PART II. SPIN-UP. Maryland: Us Army Armament research and Development Command, US, 1983. [online] Available at: http://www.dtic.mil/dtic/tr/fulltext/u2/a129094.pdf [Accessed 12 Apr. 2018].

[14] ipfs.io. (2016) Volume of fluid method [online] Available at: *https* : *//ipfs.io/ipfs/QmXoypizjW3WknFiJnKLwHCnL72vedxjQkDDP1mXWo6uco/wiki/Volume_of_fluid_method.html* [Accessed 12 Apr. 2012]

[15] Flanagan, R. (2018) Numerical Modelling Tool for Evaluation of Sloshing-Reaction Control System Coupling (SI). NUMA Engineering Services Ltd.

[16] VAN FOREEST A., DREYER M. E., AND ARNDT, T. (2011) Moving two-fluid systems using the volume-of-fluid method and single-temperature approximation. AIAA J. 49, 12 (2011), 2805-2813.

[17] NUMECAS Online Documentation platform. (2018) [online] Available at: *http* : *//portal.numeca.be/* [Accessed 12 Apr. 2012]

[18] Jiyuan Tu, Guan-Heng Yeoh ,Chaogun Liu. (2013) Computational Fluid Dynamics A Practical Approach. Oxford: Elsevier. Second edition. pp. 138-140.

[19] Jameson, A. (2003) Time-integration methods in computational aerodynamics. [online] Available at: http://aero-omlab.stanford.edu/Papers/jameson.afosr.2003.pdf [Accessed 12 Apr. 2018].

[20] Hakimi, N. (1997) Preconditioning methods for time dependent Navier-Stokes equations. Vrije Universiteit Brussel. [online] Available at: http://mech.vub.ac.be/thermodynamics/phd/Nouredine_Hakimi.pdf [Accessed 12 Apr. 2018].

9 Appendix A

European Space Agency (ESA)

European Space Research and Technology Center (ESTEC)

TEC-MPA

Driven cavity at high Reynold numbers

Numeca FINE Open v6.2 code validation

Dennis Kröger

Lunds University, Sweden
Engineering physics

Date : 05/10/2017

European Space Agency (ESA)

European Space Research and Technology Center (ESTEC)

TEC-MPA

Driven cavity at high Reynold numbers

Numeca FINE Open v6.2 code validation

Dennis Kröger

Lunds University, Sweden
Engineering physics

Date : 05/10/2017

Abstract

This work is done to validate the numerical capability of Numecas CFD software FINE Open v6.2 at high Reynold numbers. The test case used to validate the code is the driven cavity problem. The driven cavity is a widely used benchmark case.

This study will test what the highest Reynolds number is to still have a laminar flow with the FINE/Open solver. The literature is in good agreement that a Re$\leq$ 10000 results in a laminar flow. For Re$\leq$10000 the literature is divided in two. Some say it gets turbulent but others mean it can be laminar flow even above Re=10000.
E.Erturk [4] presents a steady solution up to Re=20000. The highest Reynolds number that resulted in laminar flow was found by E.M Whaba [2] that presents result that are laminar up to Re=35000.

The numerical results when using FINE Open show laminar flow Re$\leq$ 10000 which coincide well with literature [1] . For Re$\leq$10000 the solver is not amble to find a steady solution even with some added numerical dissipation and a very fine grid, 2048x2048. Some additional grid refinement was tested but no laminar results are found beyond Re=10000.

Contents

1 Introduction

The driven cavity problem is a widely used validation case for CFD solvers. It has a very simple geometry as seen in figure 1. The boundary conditions are simple Dirichlet conditions with three solid walls and a moving upper wall. All the dimensions are normalized and the upper wall velocity is set to U.

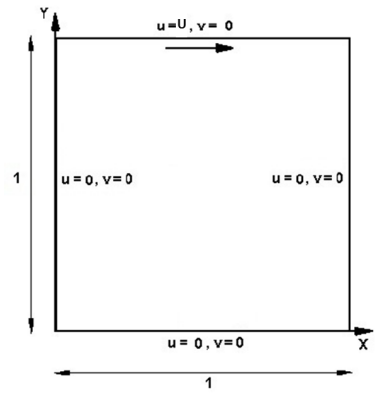

Figure 1: 2D driven cavity geometry.

Despite its simple setup, the flow can become complex, including a lot of the common flow phenomenon such as vortexes and secondary vortex.

Because this is modeled as a 2D flow there is no experimental data available for validation. The 3D experimental setup equivalent show turbulent behavior well under Re=10000. Which makes it unusable for validation. This makes it difficult to validate the numerical studies. Nevertheless it gives a feeling on how well Numecas code handles high Reynolds number flow compared to other softwares.

2 Case setup

The driven cavity is simulated for 5 different Reynold number [100,1000,5000,10000,15000]. The test plan is presented in table 1 below. For each Reynold number a mesh refinement study is performed. The different meshes run for each case are also presented in table 1.

Reynolds number	Mesh size
100	64x64 128x128 256x256
1000	128x128 256x256 512x512
5000	512x512 1024x1024 2048x2048 500x500(refined)
10000	1024x1024 2048x2048 500x500(refined)
15000	1024x1024 2048x2048 500x500(refined)

Table 1: The test plan.

2.1 Mesh

The basic mesh used for the case is produced with FINEs mesh tool, HEXPRESS. It produces an unstructured mesh with tetrahedral elements. This mesh can be seen in figure 2(a). At higher Reynold numbers a refined mesh is used in order to be able to simulate the higher velocity gradients produced. The refined mesh is shown in figure 2(b). The mesh is refined all around boundaries of the cavity.

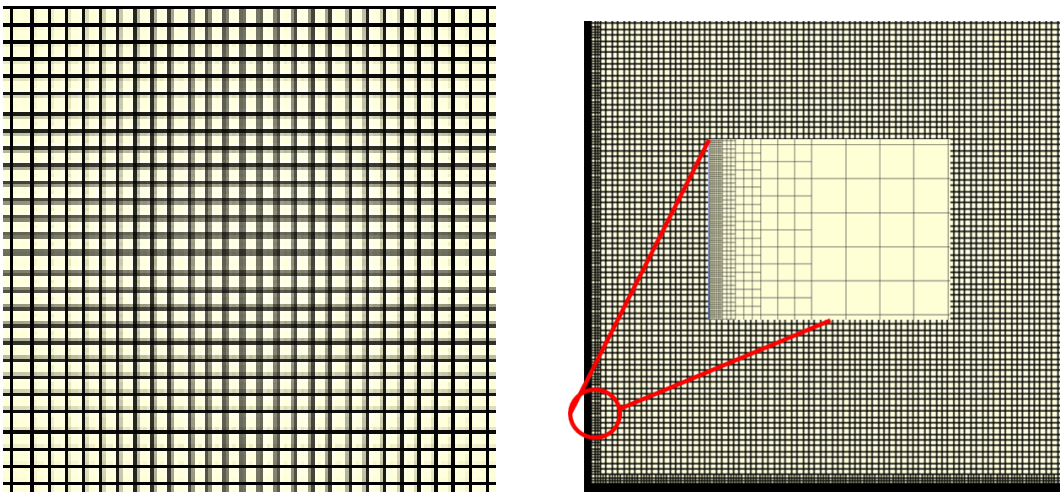

(a) Basic mesh (b) Refined mesh

Figure 2: Shows the two meshes used for simulations

2.2 Computation

FINE Open is an incompressible pressure based solver. For the cases presented in this report the following setup is used.

- Physical configuration
  - Steady solver
  - Fluid: Water
  - Flow model: Laminar Navier-Stokes
- Boundary conditions
  - Upper wall: Set x-velocity
  - All other walls: Solids
- Numerical parameters
  - Coarse grid initialization
  - Central 2nd order numerical scheme
  - Merkle preconditioning

All results presented in this report are run to a convergence of $Res = 10^{-10}$. This stopping criteria is used to make sure of an accurate representation of the flow. To be able to reach this accuracy double precision is used.

3 Results

The results are presented for the cases Re=[100,1000,5000,10000,15000]. For each Reynolds number the streamlines of the flow is shown and two velocity profiles. The first velocity profile is the x-velocity taken with a vertical line at x=0.5 from bottom to top. This line is marked as number 1 in figure 3. These velocity profiles are compared with Ghia and Shin [1].

The second velocity profile is the y-velocity at y=0.01. This line is marked as number 2 in figure 3. This additional velocity profile is studied to capture the development of the secondary vortices in the bottom corners of the cavity. For these velocity profiles no results where found in literature and are therefore just compared as a grid refinement study.

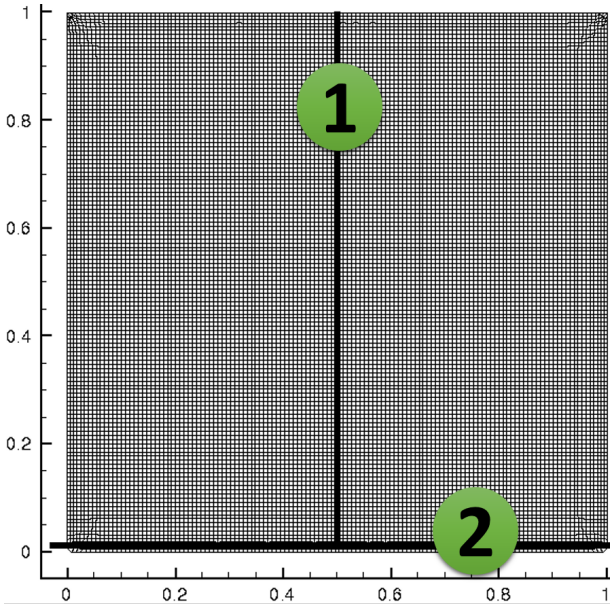

Figure 3: Shows the two lines along which the corresponding velocity profiles are extracted.

The streamlines give a physical view of the flow development with increasing Reynold number. The streamlines are hard to quantify and therefore the two velocity profiles on line 1 & 2 are extracted to quantify the accuracy of the streamlines. From the results of the velocity profiles an appropriate mesh is then chosen to present the streamlines.

3.1 Re=100

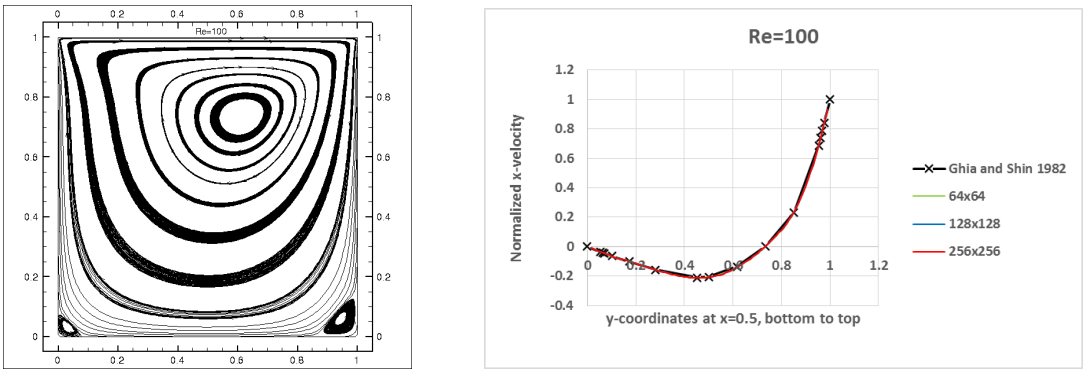

(a) (b)

Figure 4: a) The streamlines of the flow. b) The velocity profile for line 1.

Figure 4a) shows the streamlines for Re=100. The streamlines are shown for the mesh [128x128]. It can be seen that two small secondary vortices start to build in the lower right and left corner.

Figure 4b) shows the velocity profile for line 1. The velocity profile is extracted for three different fine meshes and the results are compared with Ghia and Shin [1]. From figure 4b) it seems that all three meshes give velocity profiles that coincide well with the results of Ghia and Shin [1].

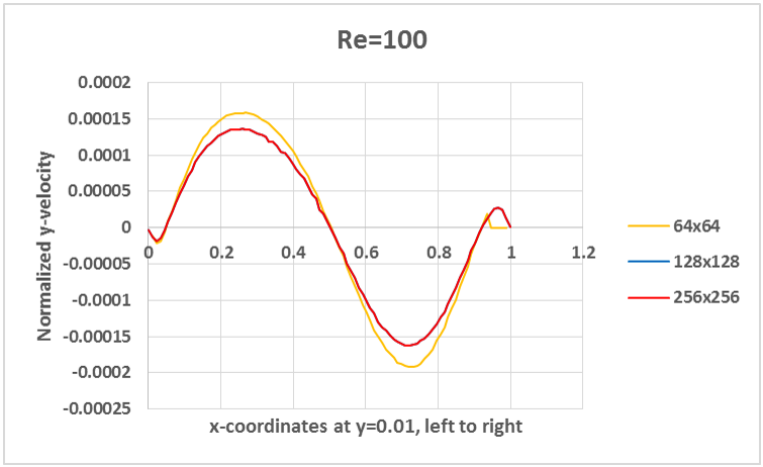

Figure 5: Velocity profile Re=100 at line 2.

Figure 5 compares the velocity profile at line 2 for Re=100 with []. Figure 5 shows that the coarse mesh of [64x64] does not give the same velocity profile as [128x128] &[256x256] which are on top of each other.

The grid refinement study of figure 4b) and 5 show that a grid of [64x64] is not fine enough grid to fully capture the flow at Re=100. Therefore the grid [128x128] was chosen to represent the streamlines.

3.2 Re=1000

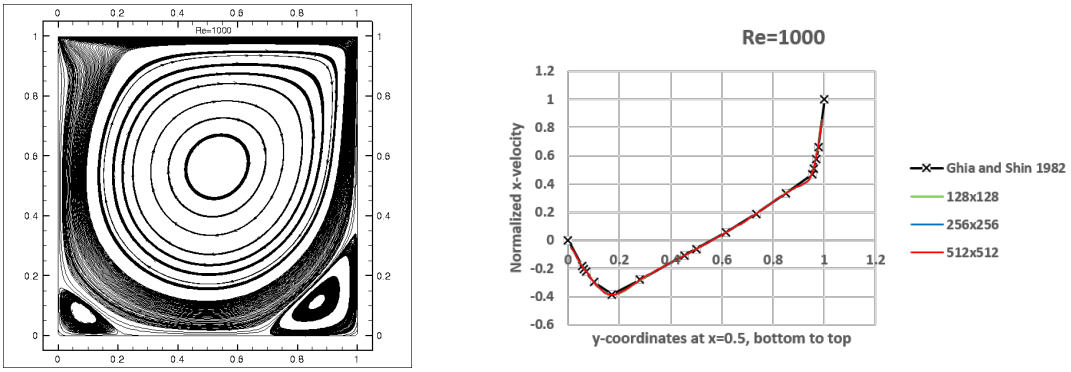

(a) (b)

Figure 6: a) The streamlines of the flow. b) The velocity profile for line 1.

Figure 6a) shows the streamlines for Re=1000. The streamlines are shown for the mesh [256x256]. It can be seen that the secondary vortices in the bottom corners that already are visible for Re=100 grow even more. A slight separation of the wall flow can be observed in the upper left corner.

Figure 6b) shows the velocity profile extracted from line 1. Similar to the Re=100 case no real difference can be observed between the three different meshes. The results are also coinciding well with [1].

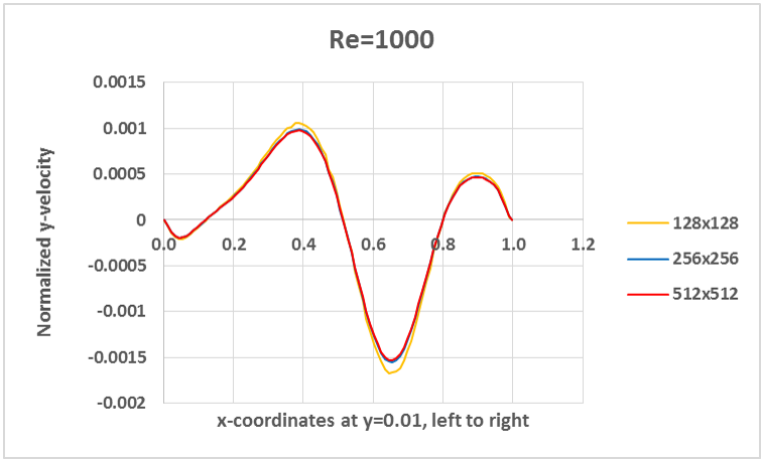

Figure 7: Velocity profile Re=1000 at line 2.

Figure 7 shows the velocity profile extracted from line 2 at Re=1000. The different meshes show that the coarse mesh of [128x128] deviates from the results of [256x256] & [512x512] which lines are on top of each other.

From these results it can be concluded that a mesh of [512x512] is fine enough to capture the flow characteristics of the driven cavity at Re=1000.

3.3 Re=5000

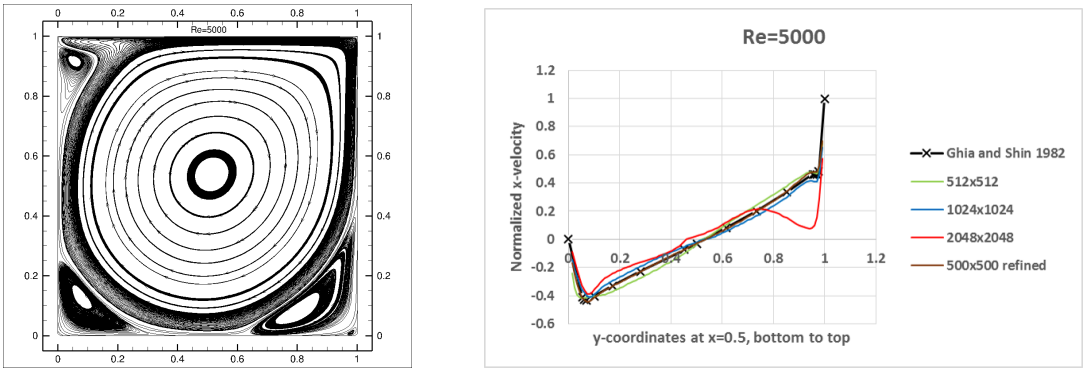

(a) (b)

Figure 8: a) The streamlines of the flow. b) The velocity profile for line 1.

Figure 8a) shows the streamlines for Re=5000. The streamlines are shown for the mesh [500x500 refined]. It can be seen that the two secondary vortices in the bottom corners have continued to grow. The vortex in the lower right corner has gained enough energy for a small tertiary vortex to build below. The flow separation in the upper left corners has also increased to a degree where a secondary vortex arises.

Figure 8b) shows the velocity profiles extracted from line 1. For the grid refinement study the additional refined grid shown in figure 2 is also used. It can be seen that the velocity profiles do not match as good as they did for lower Reynold numbers. Especially the mesh [2048x2048] shows a big deviation from the other results.

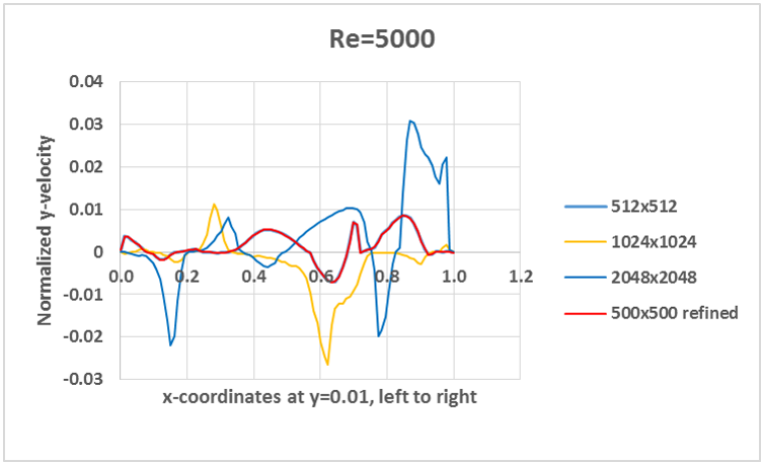

Figure 9: Velocity profile Re=5000 at line 2.

Figure 9 shows the velocity profile extracted from line 2. The profiles deviate strongly from each other. The only to meshes that coincide are [512x512] & [500x500 refined].

With these results the conclusion would be that the [512x512] mesh is a good mesh to use for this Reynold number. Because the results of even finer meshes such as [1024x1024] & [2048x2048] are not coinciding it can't be said that any mesh convergence is reached. And therefore the refined mesh is the best one for this Reynold number.

3.4 Re=10000

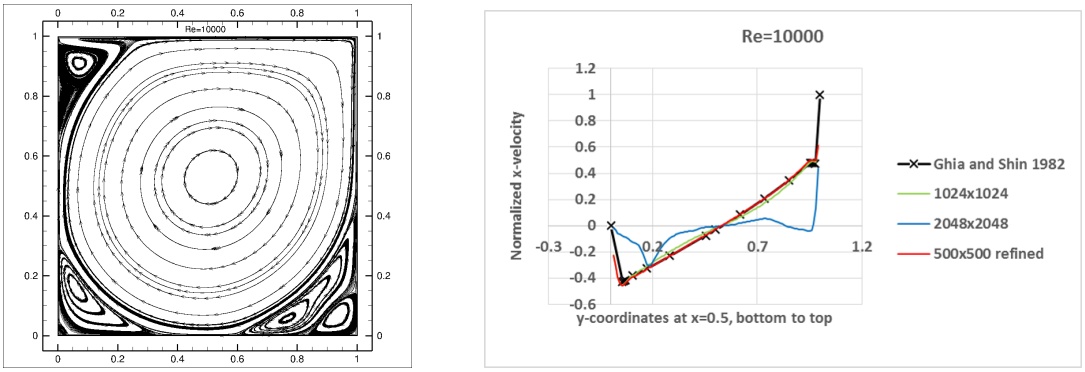

(a) (b)

Figure 10: a) The streamlines of the flow. b) The velocity profile for line 1.

Figure 10 a) shows the streamline for Re=10000. The streamlines are shown for the mesh [500x500 refined]. It can be observed that there now exist three secondary vortices, two in the bottom corners and one in the upper left corner. Additional two tertiary are forming in the bottom left and right corner.
Figure 10 b) shows the velocity profiles extracted from line 1. It can be seen that all the meshes except the [2048x2048] mesh coincide well with Ghia and Shin results. It is likely that the [2048x2048] mesh results are not numerically converged.

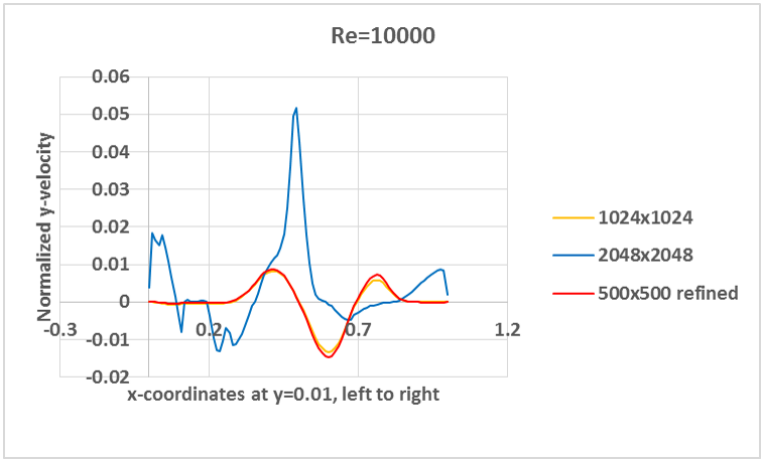

Figure 11: Velocity profile Re=10000 at line 2.

A

Figure 11 shows the velocity profiles extracted at line 2 for Re=10000. The velocity profiles of mesh [1024x1024] & [500x500 refined] coincide well whilst the [2048x2048] does not.

These results show that no mesh convergence can be shown up to a mesh of [2048x2048]. Therefore the refined mesh is the most accurate and stable mesh for this Reynold number.

3.5 Re=15000

With a Reynold number of Re=15000 FINE/Open could not converge to any stable solution. For this case the meshes [1024x1024]&[2048x2048]&[500x500 refined] are tried but no converges could be reached. Some more advanced numerical damping was added to the flow to get it to convergence with no laminar results.

3.6 Summary

The results show that steady solutions are found up to Re=10000 that coincide well with is found in literature today [1]. Above Re=10000 no steady solution can be found with a mesh resolution up to [2048x2048]. For Re≥5000 a grid refinement at the boundaries of the cavity was necessary to be able to simulate the steep velocity gradients developing at the walls.

The grid refinement studies showed that standard quadratic meshes up to a resolution of [2048x2048] is able to predict a good solution up to Re=1000.

4 Discussion

As the Reynold number increases secondary and even tertiary vortices are building up. This follows what would physical be expected. Since this is a 2D case it can't be validated through experiments.But with a thorough grid refinement study and comparison to results found in literature the results are validated to a reasonable degree.

The results from the grid refinement study are as expected for the cases Re=100 & Re=1000. For these cases a too coarse mesh gives a solution but the velocities are not accurate simulated. As the grid is refined the solution converges to one result that stays the same even when an overly fine mesh is used.

As for the cases Re=5000 & Re=10000 Some unexpected results are shown. For both cases it is shown that a coarser mesh is able to simulate the velocities in an more accurate way then a finer mesh. In both cases the [2048x2048] mesh is not able to capture the velocities correctly. Whilst a grid with a refined grid at the walls get the same velocities as the coarser mesh.

The reason for this could be that the coarser mesh works a bit like a damping factor where the smaller instabilities in the flow are overlooked and therefore lead to a more stable solution. A very fine mesh such as [2048x2048] could be more unstable because of that.

An other interesting result shown is that the velocity profile extracted from line 1 can be misleading. For the cases Re=100 & Re=1000 the velocity profile for all the different meshes are coinciding well with the results of Ghia and Shin and it could then falsely be concluded that the coarser grids are enough to simulate the flow accurately. It is first when looking at the velocity profiles extracted from line 2 that it becomes clear that the coarsest mesh is not fine enough to fully simulate the flow and velocities accurately.

In the literature Eturk [4] presents results that are laminar up to Re=21000. He uses a grid that is [601x601]. It could be that a this relatively coarse mesh is stable enough to be able to convergence to a stable solution. If the same case where to be run with a finer grid i.e. [1024x1024] there would perhaps be no stable

solution. Similar to what is shown in this report for the Re=5000 & Re=10000. This is just a hypothesis and has not been tested.

Wahba [2] presents a laminar flow up to Re=35000. This Reynolds number is achieved with a grid of [501x501]. In the simulation a stream function–vorticity formulation is adopted and a compact fourth-order-accurate central difference scheme. In this study a 2nd order central scheme was used which could one of the reasons why Wahba [2] is able to find laminar flow at higher Reynold numbers than this report shows.

References

[1] U.Ghia, K.N. Ghia, and T. Shin: High-Re Solutions for Incompressible Flow Using the Navier-Stokes equations and a Multigrid Method
`http://iopscience.iop.org/article/10.1088/1009-1963/15/8/038/meta`

[2] E.M Wahba: Steady flow simulation inside a driven cavity up to Reynolds number 35,000
`https://www.researchgate.net/publication`

[3] Hakob J.Nagapetyan Application of Wray-Agarwal Model to Turbulent Flow in a 2D Lid-Driven Cavity and a 3D Lid- Driven Box.
`http://openscholarship.wustl.edu`

[4] E.Erturk Nature od Driven Cavity Flow at High-Re and Benchmark Solution on Fine Grid Mesh.
`http://citeseerx.ist.psu.edu`